Chapter 4

Wavelet Analysis of Velocity Component

As stated in chapter 3, the major disadvantage of time and Fourier-domain parameters is that they are based on averaging over the whole records. Because the Fourier Transform does not contain any time dependence, it can not provide information on instantaneous characteristics. For instance, a delta function in time would be represented by an infinite number of Fourier components, and no information would be provided on its evolution in time. This disadvantage can be overcome in wavelet analysis, which provides an alternative way of breaking signal into its constituent components.

The wavelet transform uses local functions that are stretched and translated with varying resolutions to cover the entire time and scale content of a signal. By varying resolution, it is meant that the translation and dilations are designed to efficiently detect time variations in a signal. The wavelet transform uses short windows at high frequencies and long windows at low frequencies. Thus, it is very advantageous to characterize atmospheric turbulence, which is composed of high frequency components of short duration and low-frequency component, of long duration. Wavelet transform decomposes a signal f(t) in terms of wavelets $\psi_{\tau,a}(t)$ derived from a mother wavelet by dilations and translations, where τ and a are the translation and dilation parameters respectively. The Wavelet Transform is defined as a convolution integral of the signal and analyzing wavelet and is given by:

$$w(a,\tau) = a^{-\frac{1}{2}}\int_{-\infty}^{\infty} f(t)\psi^*(\frac{t-\tau}{a})dt \qquad (4.1)$$

The normalization factor, $a^{-1/2}$ is chosen so that all wavelets would have the same energy at each scale. $w(a,\tau)$ is the wavelet coefficients, $a^{-1/2}\psi[(t-\tau)/a]$ is the basis function or wavelets, and * is the complex conjugate.

There are many commonly used wavelets. These can be divided into two major groups, namely, continuous and orthogonal wavelets. The most commonly used continuous wavelet is the complex Morlet wavelet, which consists of a sinusoid multiplied by a Gaussian envelope. Among the most widely used orthogonal wavelets are the Daubechies wavelets with different orders. It should be noted that when applying wavelets in signal analysis, they must be discretized and that discrete wavelet transforms are not always orthogonal. Rather, the orthogonality is based on very special choices of wavelet basis functions. One way to discretize the time-scale parameters a and τ is to let $a=2^j$ and $\tau=k2^j$, where the indices k and j are integers. Note that, when k and j increase linearly, a and τ change exponentially. Based on this discretization, a true orthonormal basis will be obtained for special choices of wavelet functions.

Because the scales are analyzed only at integer powers of two or by octave, the orthogonal decomposition may not yield the most meaningful scale analysis. On the other hand, they are more desirable in decomposition and in reconstruction of

Table 4.1 Scale index and corresponding scale duration and frequency range

Scale index (m)	Number of wavelets	Scale duration (s)	Freq. Range (Hz)
M=-1	Signal mean value	-	-
M=0	1	16.384	[0.061, 0.122]
M=1	2	8.192	[0.122, 0.244]
M=2	4	4.096	[0.244, 0.488]
M=3	8	2.048	[0.488, 0.977]
M=4	16	1.024	[0.977, 1.95]
M=5	32	0.512	[1.95, 3.91]
M=6	64	0.256	[3.91, 7.81]
M=7	128	0.128	[7.81, 15.6]
M=8	256	0.064	[15.6, 31.3]
M=9	512	0.032	[31.3, 62.5]
M=10	1024	0.016	[62.5, 125]
M=11	2048	0.008	[125, 250]
M=12	4096	0.004	[250, 500]

time series. Consequently, the function f(t) can be represented by a weighed sum of basis functions. The relative contributions to the mean square value of a signal from all scales are given by the wavelet coefficients. In this work, Daubechies orthogonal wavelets are applied to obtain the wavelet coefficients, decomposed wavelet levels and the energy distribution among different scales and their time variations.

The data analyzed in this chapter are velocity time series obtained at the height of 7.92cm in the wind tunnel and with the fan speed in the wind tunnel set at of 800. The u- and v- components are measured with an X- hot wire anemometry system. The sampling frequency is set at 4000 Hz and the sampling period is 180 seconds. So the total data points in each file is 720,000. In order to compare the results to field data results obtained from WERFL at Texas Tech, which has a sampling frequency of 10Hz and a sampling period of 819.2 seconds, the wind tunnel data is re-sampled every eighth point, giving a time series with a sampling frequency of 500Hz. From these records, 10 segments, each containing 8192 points, are used in the wavelet analysis. Experiment conditions were maintained the same during the measurement, therefore, the time series of each segment should reveal similar characteristic. The average of results of the 10 segments is used to reduce errors. With a sampling frequency of 500Hz and 8192 samples in each segment, the largest scale that can be characterized is given by m=0 and corresponding to 0.050Hz; and the smallest scale is given by m=12 and corresponding to 250 Hz. Table 4.1 gives the scale index m, scale duration in seconds and frequency range covered by each scale in our analysis.

Figure 4.1 to 4.8 show the time series of velocity fluctuations and the corresponding wavelet coefficients for both u- and v- component for scales from m=1 to 12 (0.122 to 500Hz) for the different configurations discussed in Chapter 2. These coefficients give a representation of how energy is distributed among different scales and how it varies with time. It is obvious from these figures that scales of both u- and v- component are highly intermittent. By intermittency, it is meant that, over short time periods, the scales may have significant contribution to the total turbulence energy. Locations on the time axis associated with high-energy event may appear randomly during the whole period, and may exist only within limited scales.

By comparing wavelet coefficients of velocity fluctuations in configuration #2 as shown in figure 4.2 to those of configuration #1 in figure 4.1, we notice that, there is an apparent increase of level of fluctuations for both u- and v- components, as a result of introducing trip and big spires at the entrance of the bare tunnel. For the u- component and for scales between m=2 and 7 (0.244Hz<f<7.81Hz), maximum amplitude and level of energy of the wavelet coefficients for u- component have consistently increased as a result of addition of these elements. As for the larger scales between m=8 and m=12 (15.6 Hz<f<250 Hz), the level of energy is about the same for both configurations. However, the maximum amplitudes for these scales observed in configuration #2 are almost twice higher than those observed in configuration #1. This indicates higher energy events for smaller scales in configuration #2 than in configuration #1. At the same time, comparison of v- components of these two configurations reveals similar characteristics. Moreover, the extent of increase for v- component in configuration #2 is much higher than that of u- component and the scales, which have higher wavelet coefficients, cover a wider frequency range (1< m<8 or 0.122 Hz<f<15.6 Hz). Thus, by adding big spires and trip at the tunnel entrance, the level of energy of large scales (up to 7.81Hz), relative to the smaller scales, can be controlled. These elements seem to affect the v- component more significantly.

In comparison to configuration #2, configuration #3 has an additional row of small spires just upstream of the model. This configuration change is reflected clearly in the comparison of the u- and v- time series in both configurations (figures 4.2 and 4.3). The levels of fluctuations of the u- and v- components are about the same for the two configurations. However, the fluctuations in configuration #3 seem to have higher frequency variations than in configuration #2. This indicates a higher energy level in smaller scales. Comparison of wavelet coefficients, for scales between m=3 and 7 (0.488 to 7.81Hz), show that for the u-component, they have lower magnitude in configuration #3 than in configuration #2. This difference is more obvious for large scales between m=3 and 4 (0.488 to 0.977Hz). For scales with m larger than 8 (frequencies above 15.6 Hz), the maximum value of the wavelet coefficients and level of energy in configuration #3 are consistently higher than those in configuration #2. This change of distribution for wavelet coefficients indicates that the level of energy of smaller scales relative to larger scales can be controlled by adding a row of small spires just upstream of the model. These spires affect both the u- and v- components to a similar extent.

In both configurations #4 and #5, baffle floor roughness elements are introduced. However, configuration #5 has an additional row of small spires located upstream of the model. Time series comparison of these two configurations (Figures 4.4 and 4.5) with that of bare tunnel reveals that, by adding baffles, the level of fluctuations of both u- and v- components is increased. This increase is more obvious for the v- component. The effect of adding the baffles is similar to the effect of adding big spires. Wavelet coefficients comparison shows that the values of large to intermediate scales with m between 2 and 7 (0.244 to 7.81) are significantly higher and the effects in v- component are more pronounced than in u- component.

Configurations #6 and #7 both have conventional floor roughness. Configuration #7 has an additional row of #7 spires as explained in Chapter 2. Comparison of time series of the u- component in these two configurations shows that small scale energy is higher in configuration #7 than in configuration #6. At the same time, large scales between m=1 and 5 (0.122 to 1.95) in configuration #7 have consistently lower wavelet coefficients than those in configuration #6. The maximum magnitude of the wavelet coefficients of their intermediate scales represented by scales between m=6 and 7 (3.91 to 7.81Hz) are about the same. Configuration #7 has higher values of wavelet coefficients among smaller scales as represented by m=8 to 12 (15.6 to 250Hz).

Comparison of the time series of the v- component in configuration #6 and #7 shows that, there is more small scale activity in configuration #7 than in configuration #6. The wavelet coefficients in configuration #6 have higher energy in comparison with configuration #7 for large scales between m=2 and 5 (0.244 to 1.95Hz). On the other hand, the wavelet coefficients in configuration #7 are higher for the intermediate scales between m=7 and 8 (7.81 to 15.6Hz). For small scales, between m=9 and 12 (33.3 to 250Hz), the relative variations between these two configurations are not consistent. The above discussion indicates that, by adding #7 spires to conventional roughness, the wind tunnel tends to generate turbulence with velocity fluctuations having higher frequencies rather than having larger fluctuating magnitude. At the same time, small-scale activities are enhanced, at the expense of the energy of the larger scales. This is more obvious in u- component than in the v- component.

Configuration #8 has a row of small spires at the upstream location with respect to the model prism. It has also a row of big spires. However, different from previous configurations with their location at tunnel entrance, the big spires in configuration #8 are placed in the middle of the test section. In addition, the shape and number of the big spires in the row are different from previous ones. Among all other configurations, configuration #3 is closest to configuration #8 with respect to the experimental setup. Comparison of the time series as shown in figures 4.3 and 4.8 indicates that, the change in big spire location has some influence on both u- and v- components, but with different extents. The fluctuations of u- component in both configurations appear to be similar, however, for v- component, configuration #8 has much larger fluctuations than configuration #3. Figures 4.3 and 4.8 also show that, the wavelet coefficients in intermediate to large scales are about the same for both components in both configurations. For the u- component, these scales cover a range for m above 5 (>1.95 Hz), and for v- component, the range is for m above 4 (>0.488 Hz). This implies that, the location of big spires in wind tunnel simulations does not influence the energy with frequencies higher than 1.5 Hz. However, this change of location has some influence on energy levels of large-scales. The wavelet coefficients of u- component in scales between m=1 to 4 (0.122 to 0.977Hz) in configuration #8 are larger than those in the equivalent scales in configuration #3. On the other hand, values of wavelet coefficients of v- component in large scales in configuration #8 are smaller than those in configuration #3. Therefore, moving big spires to different locations can control energy level of large scales. Placing these spires at the entrance in comparison to just upstream of the model leads to lower u- component activity but enhance v- component activity.

Based on above wavelet representation and in order to examine time variations, three parameters, scale energy, intermittency factor and percentage of intermittent energy are defined to characterize the turbulence for different configurations. The *scale energy* is defined as the percentage of the total energy contained in each scale. The *intermittency factor* is defined as the percentage of the time a scale is in its higher state. The *intermittency energy* is defined as the percentage of the energy of each scale that is contained during the high-energy periods. These three quantities not only give relative energy levels among different scales or frequency ranges, but also give a measure of the time variations in the energies of these scales. Figures 4.9 to 4.16 show these three quantities for all the configurations. By comparing these results, it is expected to determine the effect of each configuration setup on the inermittency level and time-varying characteristics of turbulence in each setup.

Configuration #1 is the bare tunnel. Its intermittency parameters are plotted in Figure 4.9 and 4.10. It is noted that for u-component, most of the energy is contained in scales between m=4 and 10 (0.977 to 125Hz), with each containing 10% to 16% of the total energy. The scales with m=8 (15.6Hz) contains the highest percentage energy, which is about 16%. The energy between scales represented by m=4 and 10 (0.977 to 125Hz) is relatively equally distributed. For intermittency factor, larger scales, between m=2 and 3 (0.244 to 0.488Hz), have a value about 25%. All other scales have a slightly lower similar value at about 20%. The percentage of intermittency energy of all scales for bare tunnel is about 60% for all scales. Therefore, about 60% of the scale energy appears in about 20% of the total time for all scales, though there is significance different with respect to the value of scale energy among all scales.

As for the v- component, the results presented in figure 4.10 show that most of the energy is contained in the small scales between m=8 and 12 (15.6 to 500Hz). For scales with m larger than 5, the intermittency factor is about 20%, and the corresponding intermittency energy is about 60%. We should note that scales between m=8 to 12 (15.6 to 500Hz) contain most of the total energy.

Configuration #2 is the bare tunnel plus big spires. Figures 4.9 and 4.10 show that, the intermittency parameters for configuration #2 are different from those of configuration #1. The most obvious difference is the uneven distribution of energy among scales. For both u- and v- component, one scale, m=5 for u-component and m=6 for v- component, seems to contain more energy than the other scales. By comparison, it is noted that, the energy seems to be shifted from small scales to large scales as a result of adding the row of big spires. The shift is more obvious in v- component than in u- component. Another difference between configuration #2 and configuration #1 is that, the overall energy distribution among scales is similar between u- and v- components. The intermittency factors for scales between m=4 to 7 (0.977 to 7.81Hz) are about 17%. The intermittency energy is about 60%. Therefore, the intermittency events among these scales are about the same. Though the intermittency events in other scales may be relatively larger when considering both the values of intermittency factors and the intermitency energy, because of the low scale energy, they are not significant. By comparison between configuration #2 and #1, it is shown that, by adding big spires, energy is shifted from small scales to large scales, intermittency factors of larger scales decrease, the intermittency energy is maintained the same. This indicates an enhancement of the intermittency activities. The results of the vcomponent are shown in Figure 4.10. The characteristics are similar to those of u- component.

The intermittency parameters of configuration #3 are shown in figure 4.9 and 4.10. It is noted that in configuration #3, energy of u- component is shifted from large scales to small scales compared with configuration #2. Most of the energy is contained in scales between m=5 and 10 (1.95 to 62.5Hz). Among these scales, m= 8 and 9 (15.6 to 31.3Hz) contain the highest percentage energy with values about 15%. The intermittency factors of scales between m=3 and 5 (0.488 to 1.95Hz) are about 12%, and similar to those in configuration #2. However, configuration #2 has a much higher scale energy. The intermittency energy for these three scales is about 40%, lower than that in configuration #2. This indicates that, large scale intermittency activity is stronger in configuration #2 than in configuration #3 for u- component. Among smaller scales between m=8 and 10 (15.6 to 62.5Hz). Scale energy of m=8, 9, and 10 (15.6 to 62.5Hz) of configuration #3 is consistently higher than those in configuration #2, while the intermittency factor and intermittency energy are about the same. Therefore, the small scale intermittency activity of configuration #3 is stronger than that of configuration #2.

Intermittency characteristics of the in v- component (figure 4.10) are similar to those of the u- component. Most of the energy is contained in scales between m=5 to 10 (1.95 to 62.5Hz), with values about 12%. Among these scales, the energy distribution is quite even. The intermittency factors for scales between m=5 and 7 (1.95 to 7.81Hz) is about 15%, which are similar to those in configuration #2. Intermittency energy of these three scales is about 60%, which is about the same as that in configuration #2. Therefore, it could be concluded that, introducing small spires tends to shift energy from larger scales to smaller scales for both u- and v- components. At the same time, intermittency activity is decreased in larger scales and increased in smaller scales.

Intermittency parameters of u- component of configuration #4 are shown in figure 4.11. We notice that, most of the energy of u- component is in the scales between m=3 and 8 (0.488 to 15.6Hz). The intermittency factors for scales between m=3 and 5 (0.488 to 1.95Hz) are from10% to 20%. The intermittency factors for scales above 6 (>3.91 Hz) are about 15%. The corresponding intermittency energy for m=3, 4 and 5 (0.488 to 1.95Hz) is 30%, 60% and 25%. The intermittency energy for scales above m=6 (3.91Hz) is all maintained at about 60%. Therefore, the intermittency activity is strong among all scales with m larger than 3 (0.488Hz) except for scale with m=5 (1.95Hz) with a value of intermittency energy about 25%.

Intermittency parameters of v- component of configuration #4 are shown in figure 4.12. Compared with u- component, energy of v- component is more evenly distributed among all scales. Most of the energy is in scales between m=4 to 9. Percentage intermittency factors between scales m=4 and 9 (0.977 to 31.3Hz) are all about 15%. The value of intermittency energy for scale with m=4 (0.977Hz) is the lowest, which is about 35%, while the intermittency energy values of the other scales are all maintained at about 55%.

As for configuration #5, its intermittency parameters are plotted in Figure 4.11 and 4.12. We notice that, in comparison with the results of configuration #4, energy of both u- and v- components is shifted from large scales to small scales. However, most of the energy is still distributed among scales between m= 4 to 9 (0.977 to 31.3Hz), and with values between 10% to 16%. For scales between m=4 and 6 (0.977 to 3.91Hz), the intermittency factor and intermittency energy are about the same.

Comparison between configuration #4 and #5 indicates that, by adding a row of small spires, the energy is shifted from large scales to small scales, the intermittency events are decreased in large scales and intermittency events in small scales are increased. This effect is true for both u- and v- component. These results verify what we have already obtained by the comparison between configuration #2 and #3.

Figures 4.13 and 4.14 show the intermittency parameters of configuration #6. It is noted that, most of the energy of u- component is distributed among scales between m=5 and 8 (1.95 to 15.6Hz), and between 5 and 10 (1.95 to 62.5Hz) for v- component. Energy distribution is relatively even for both components with a value of 15% for u- component, and 12% for v- component. The intermittency factors of u- component for scales between 4 and 12 (0.977 to 250Hz) are about 17%, and the corresponding intermittency energy is about 60%. Therefore, for scales containing most of the energy, about 60% of the scale energy appears within about 15% of the time.

Comparing the intermittency parameters in configuration #7 with configuration #6 (figures 4.13 and 4.14), it is noted that energy is shifted from large scales to small scales for both u – and v- components as a result of adding #7 spires. Most of the energy for the u- component is distributed between scales with m between 5 and 10 (1.95 to 62.5Hz). For the v- component, scales with m between 6 and 11 (3.91 Hz to 125 Hz) contain most of the energy. Comparing the intermittency factor and intermittency energy of these two configurations, there is no significant difference. Therefore, adding #7 spires decreases the intermitency events in large scales, and increases the intermittency events in small scales. It is also noted that the extent of the increase of small scale energy for the v- component is much larger than that of u- component. Therefore, the #7 spires are especially effective in increasing small-scale activities for the v- component.

Observing intermittency parameters of configuration #8 shown in figures 4.15 and 4.16, most of the energy are distributed between scales m=4 and 9 (0.977 to 31.3Hz) for both u- and v- components. About 60% of the scale energy appears in about 15% of the time for scales with m above 5 (1.95Hz) for both u- and v- components. Comparing the intermittency parameters of configuration #8 with configuration #3, no noticeable difference with respect to intermittency events in small scales with m above 7 (7.81Hz) is observed. However, for large scales, scale energy of configuration #8 is higher than that of configuration #3. Therefore, the intermittency events are stronger in configuration #8 than in configuration #3 for large scales between m=2 and 5 (0.244 to 1.95Hz).

The wavelet analysis based on the three derived parameters, scale energy, intermittency factor and intermittency energy is presented. The results show that, the effect of introducing small spires is to shift energy from large scales to small scales. The intermittency activity is decreased in large scales and increased among small scales. The conclusion is in accordance with the result obtained from spectral analysis. Its advantage over spectral analysis is that it provides information of the intermittency activity, which shows that, for both u- and v-components, most of the energy of different scales appears in very short periods of time.

Overall, all configurations maintain similar intermittency events in small scales while different configurations may have different intermittency events in large scales. Absolute energy and percentage energy distribution among scales are not necessary the same. However, they can be controlled by different configuration setups.

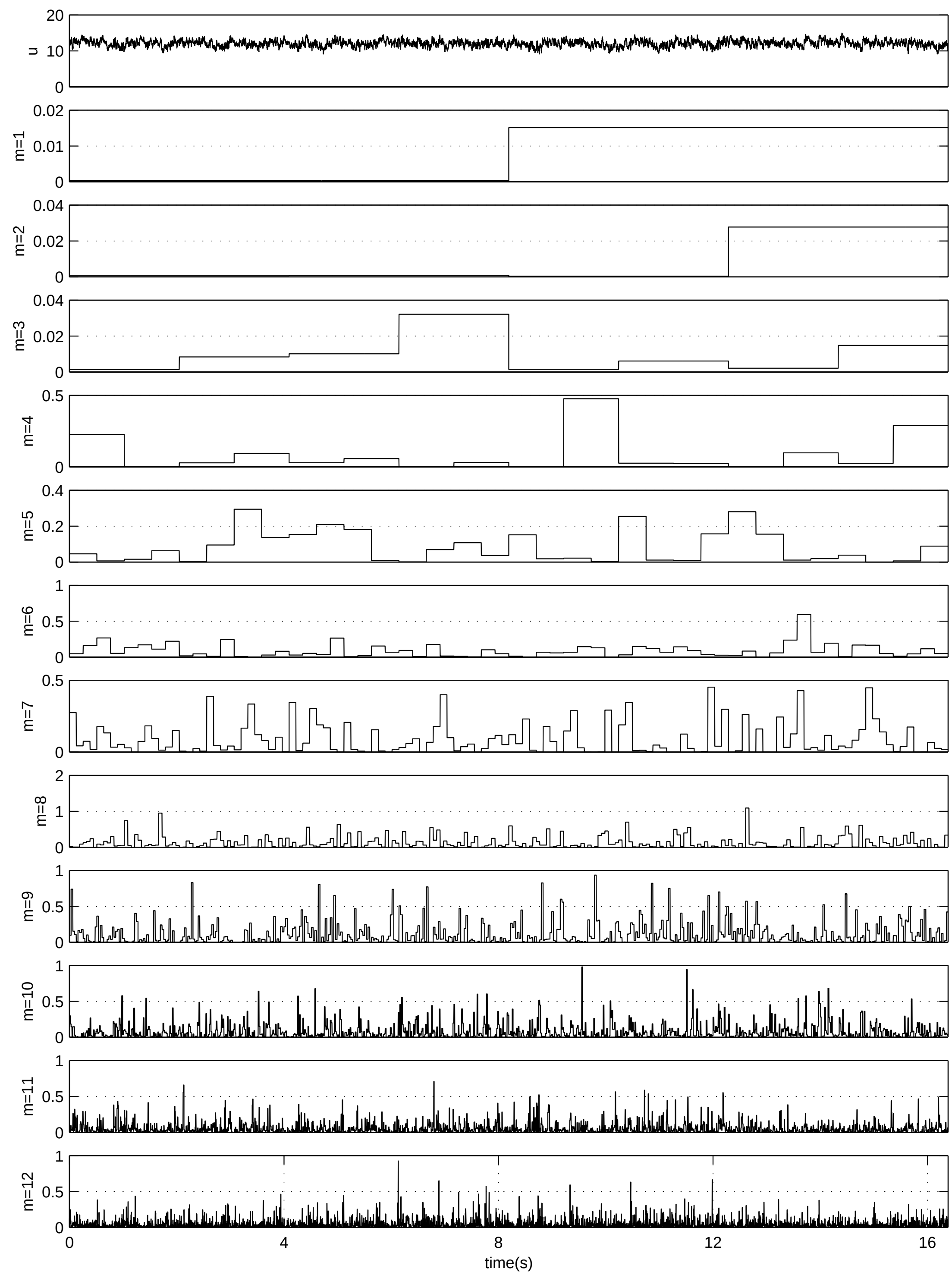

Figure 4.1(a) Wavelet coefficients of u- velocity component of Configuration #1

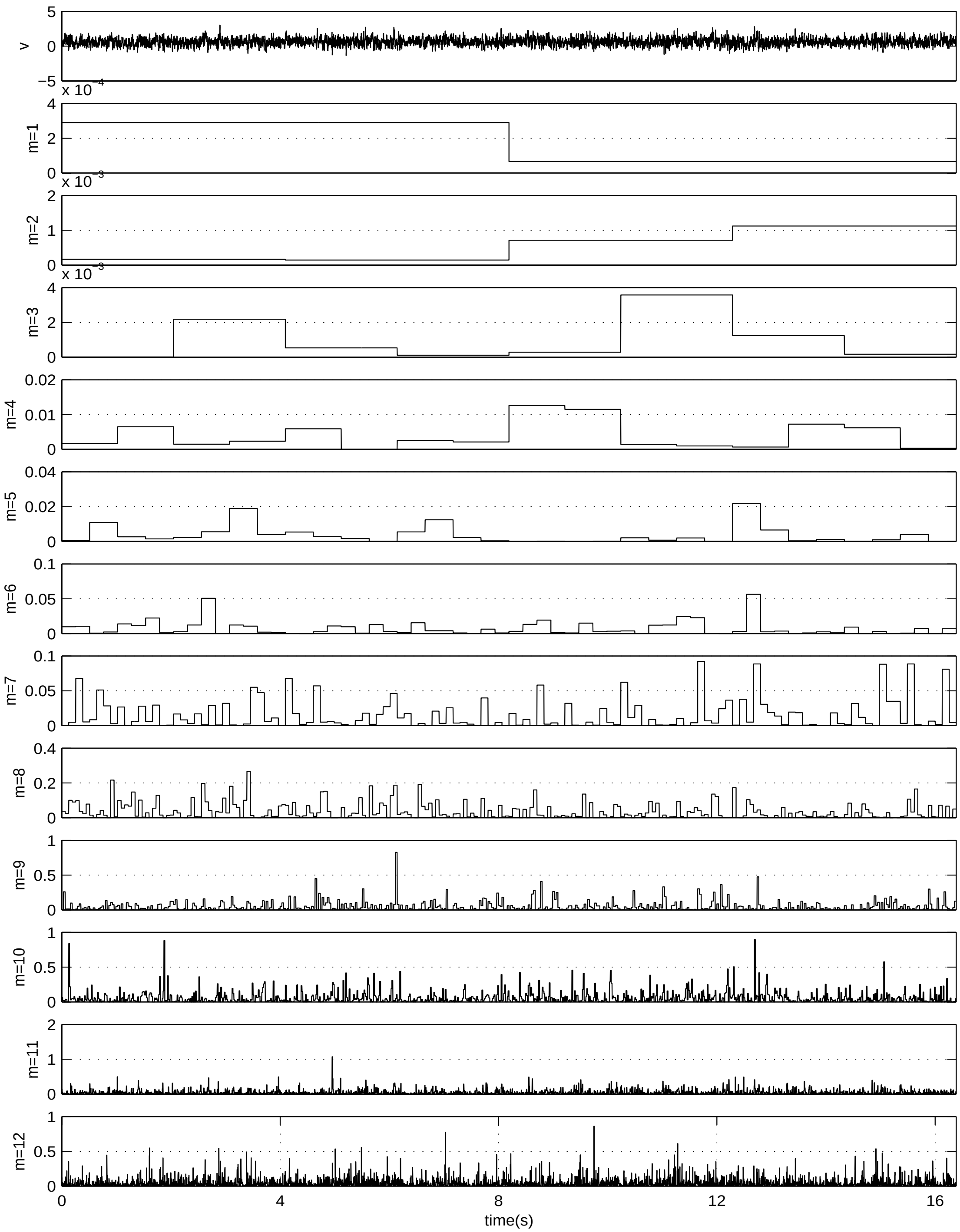

Figure 4.1(b) Wavelet coefficients of v- velocity component of Configuration #1

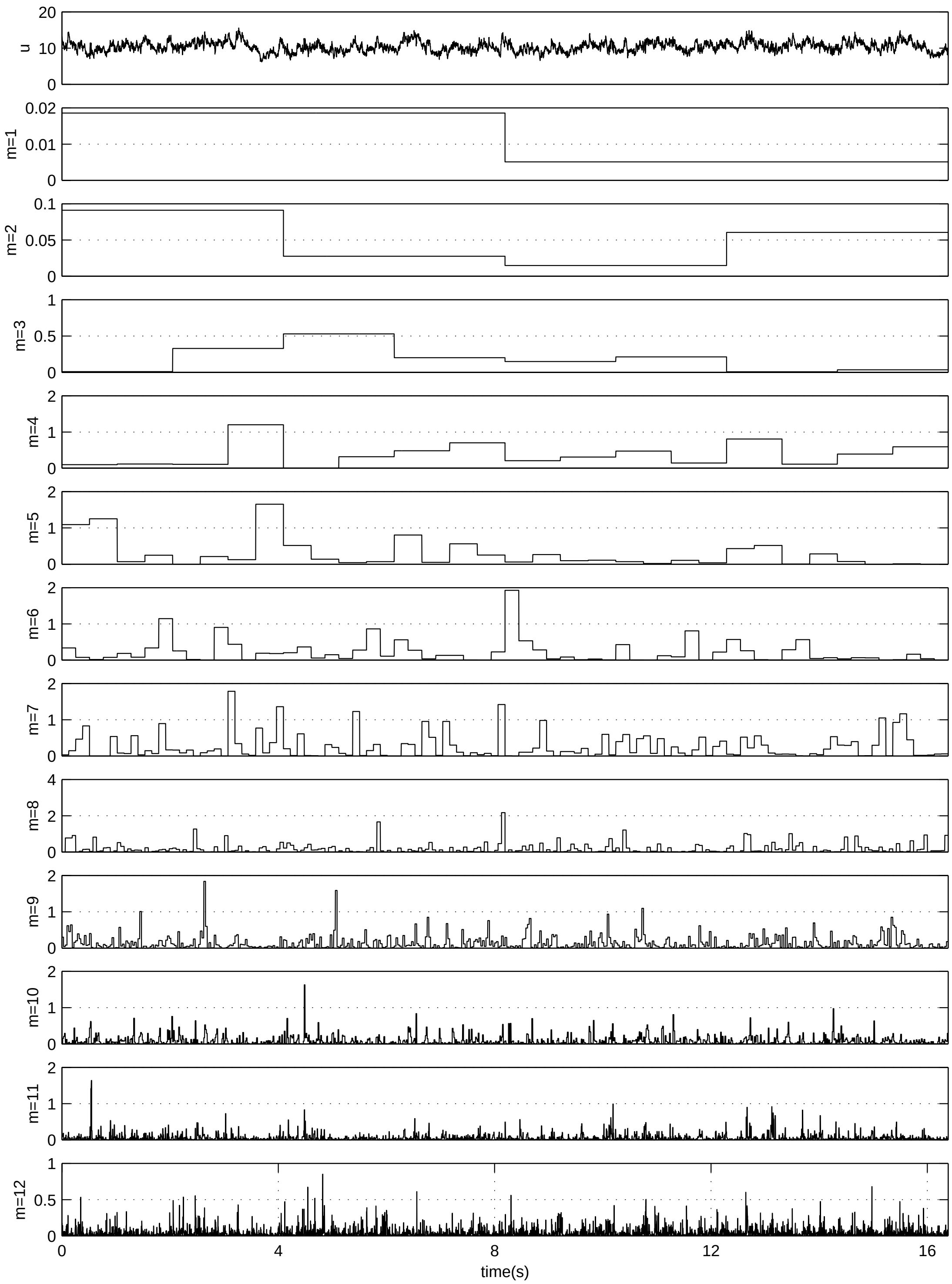

Figure 4.2(a) Wavelet coefficients of u- velocity component of Configuration #2

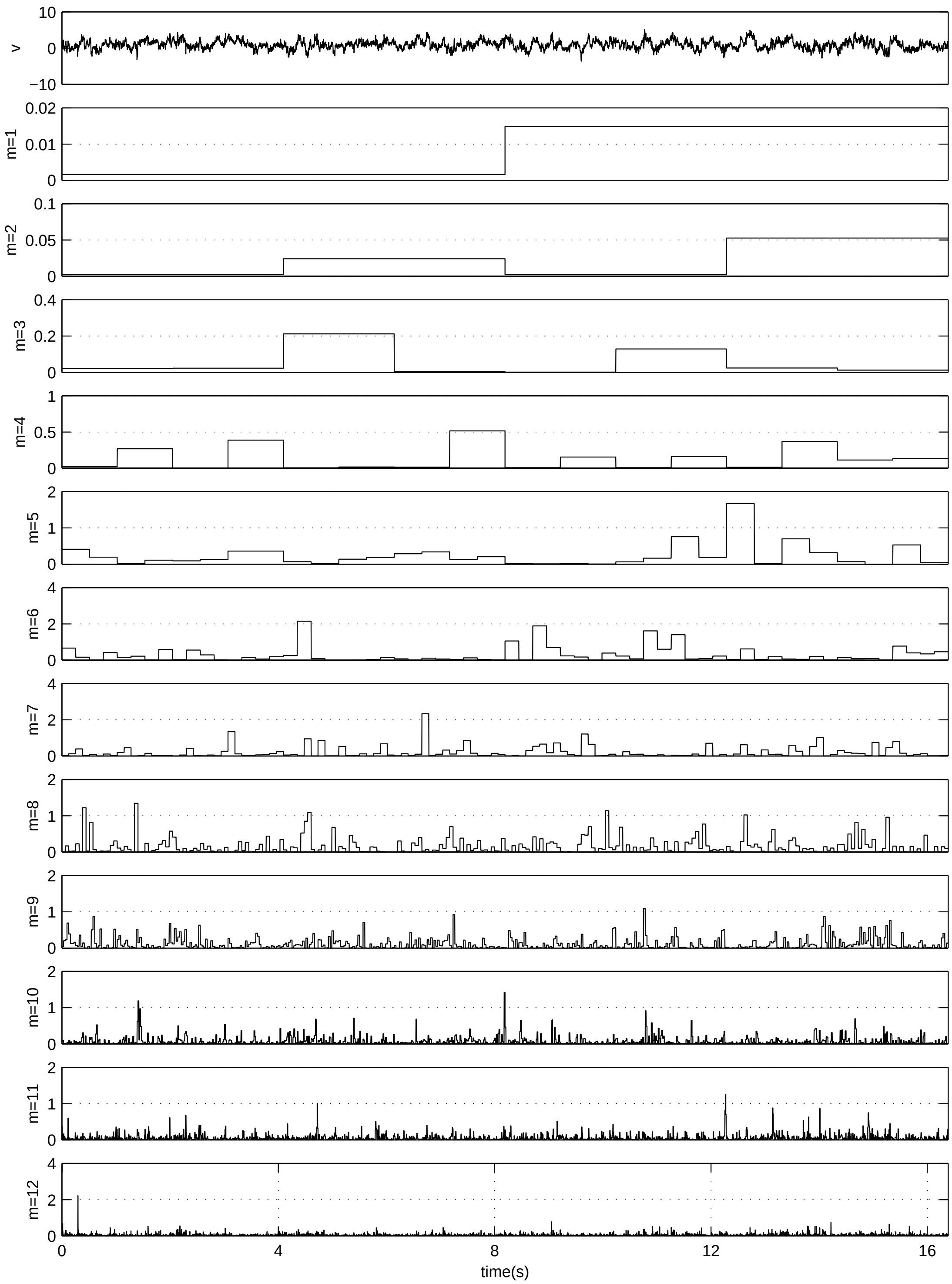

Figure 4.2(b) Wavelet coefficients of v- velocity component of Configuration #2

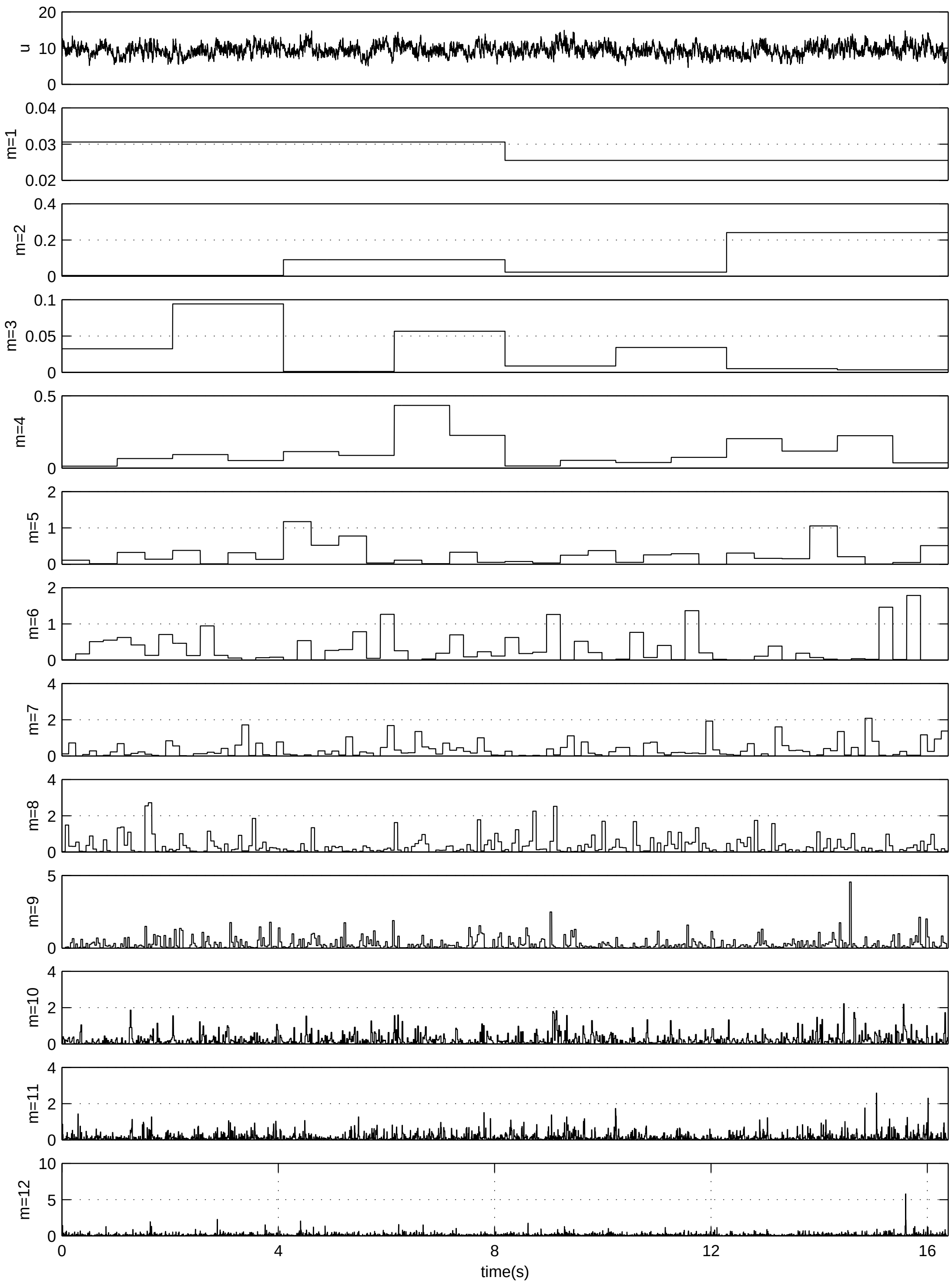

Figure 4.3(a) Wavelet coefficients of u- velocity component of Configuration #3

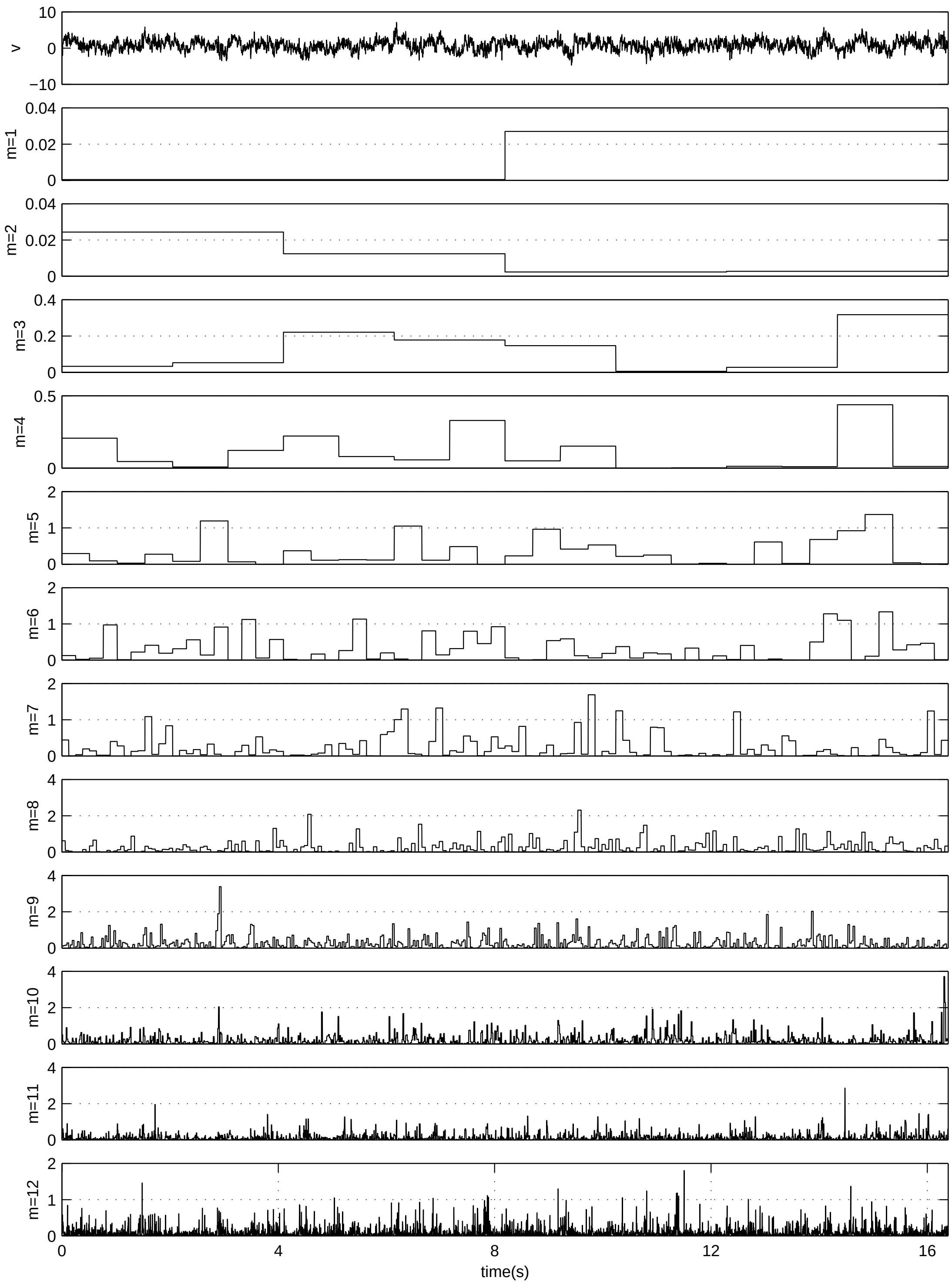

Figure 4.3(b) Wavelet coefficients of v- velocity component of Configuration #3

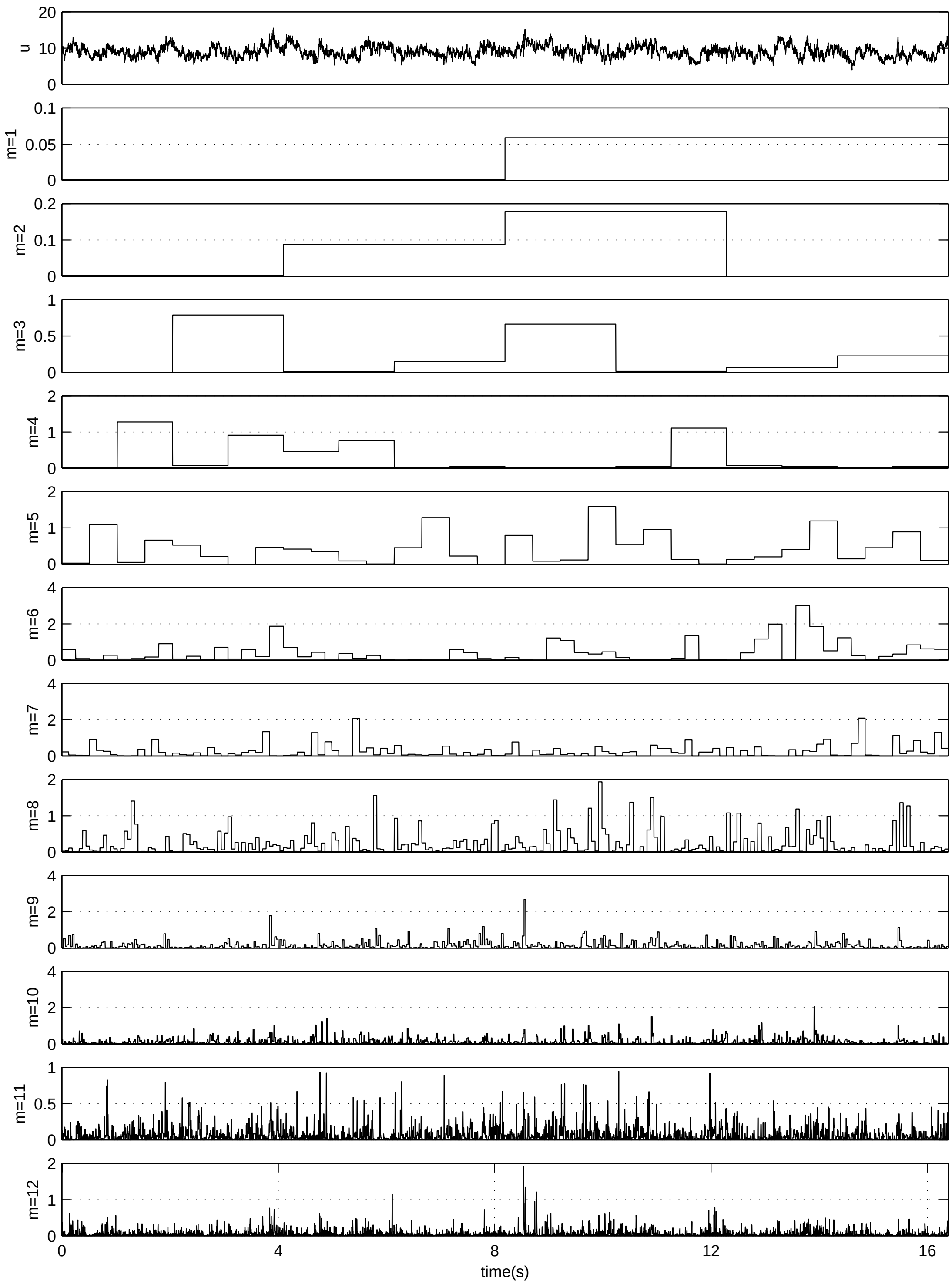

Figure 4.4(a) Wavelet coefficients of u- velocity component of Configuration #4

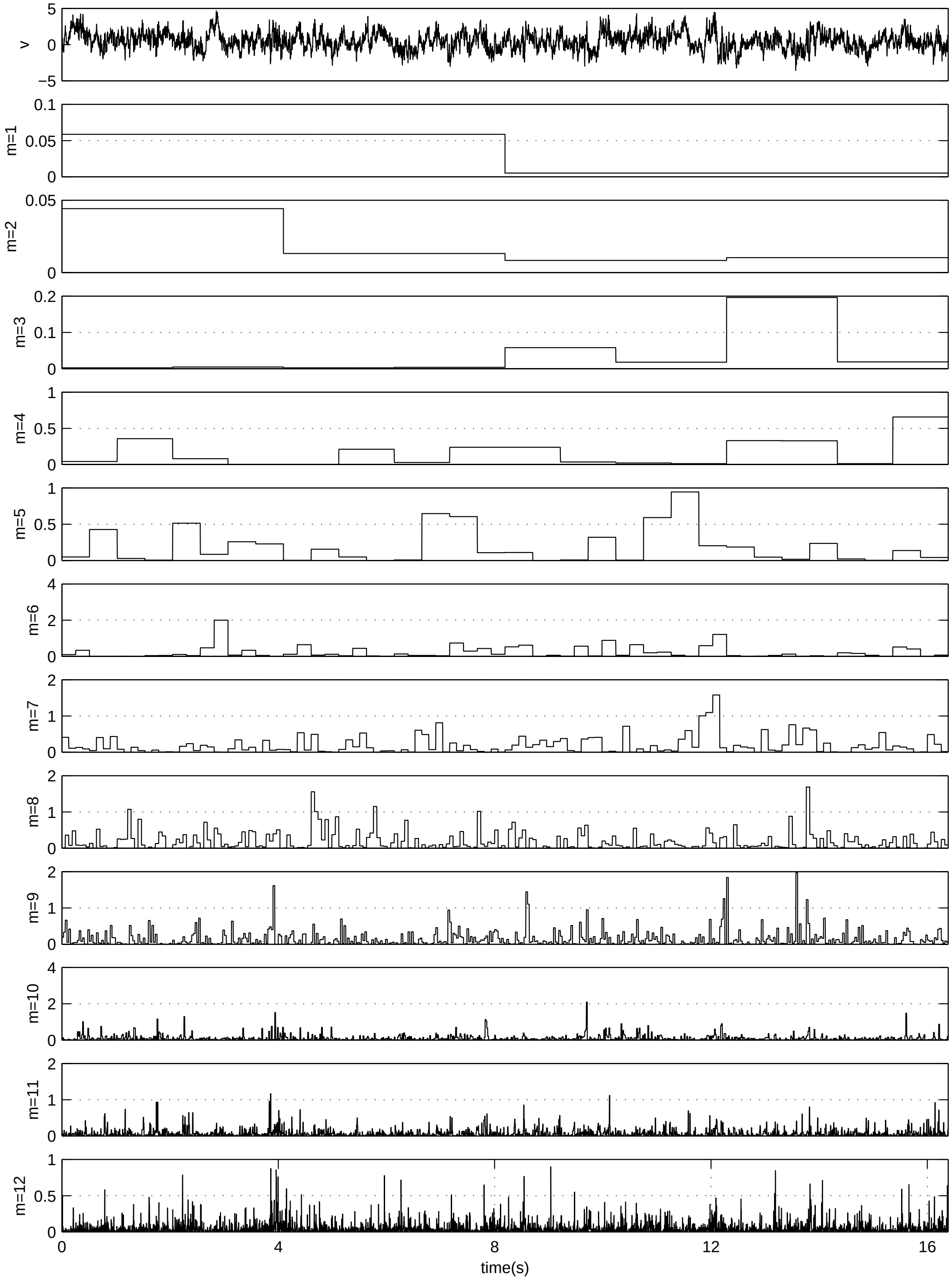

Figure 4.4(b) Wavelet coefficients of v- velocity component of Configuration #4

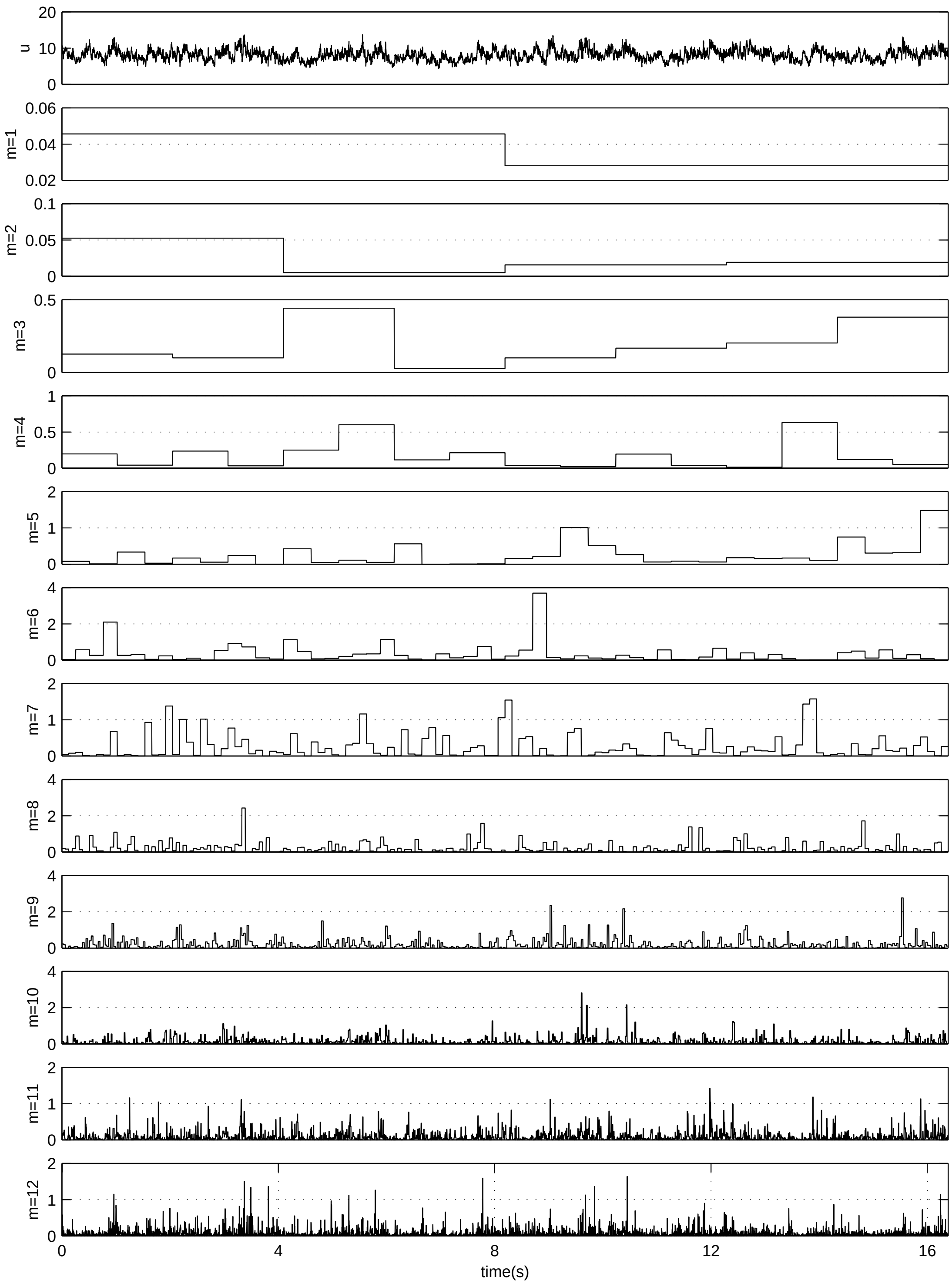

Figure 4.5(a) Wavelet coefficients of u- velocity component of Configuration #5

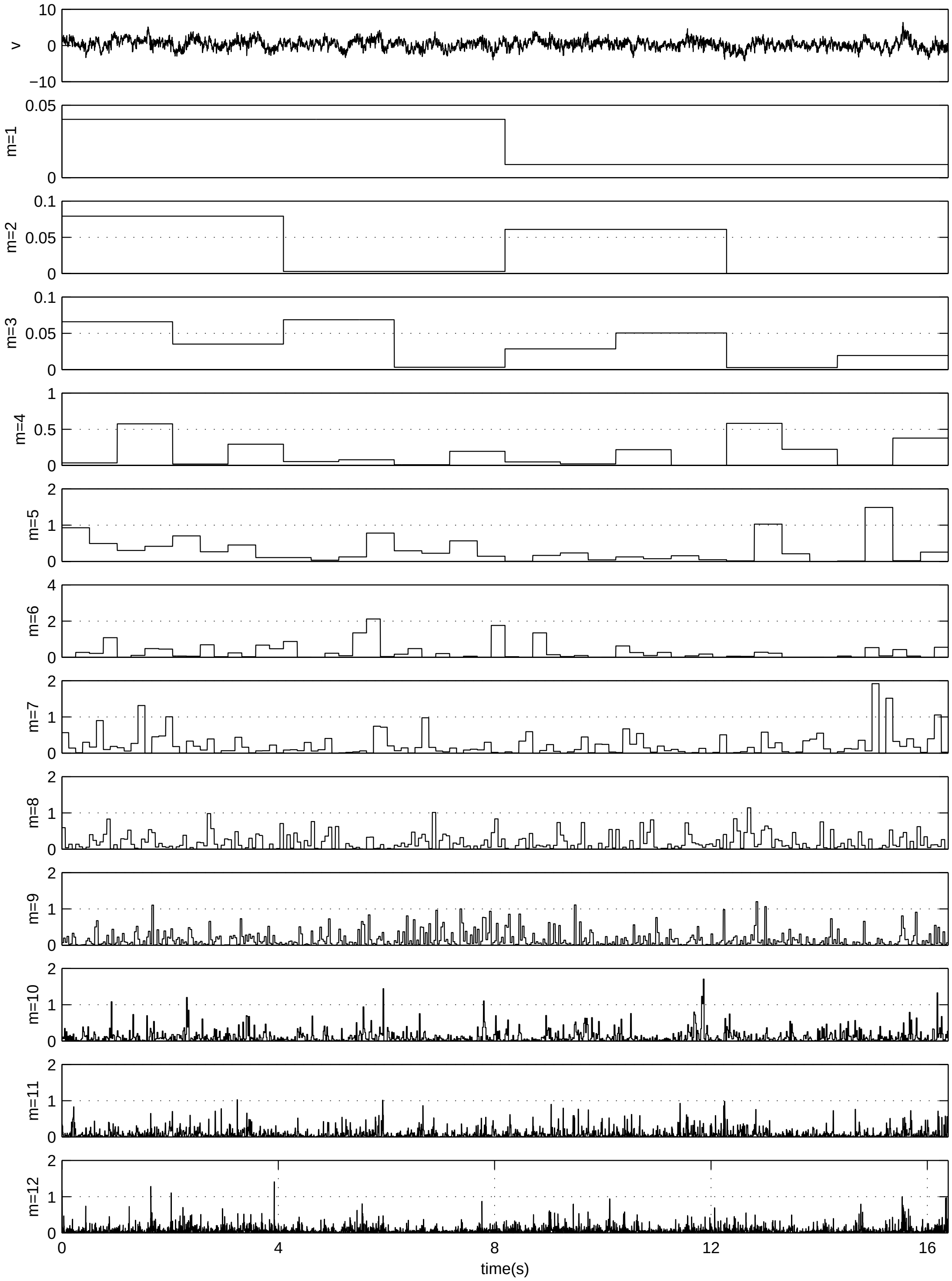

Figure 4.5(b) Wavelet coefficients of v- velocity component of Configuration #5

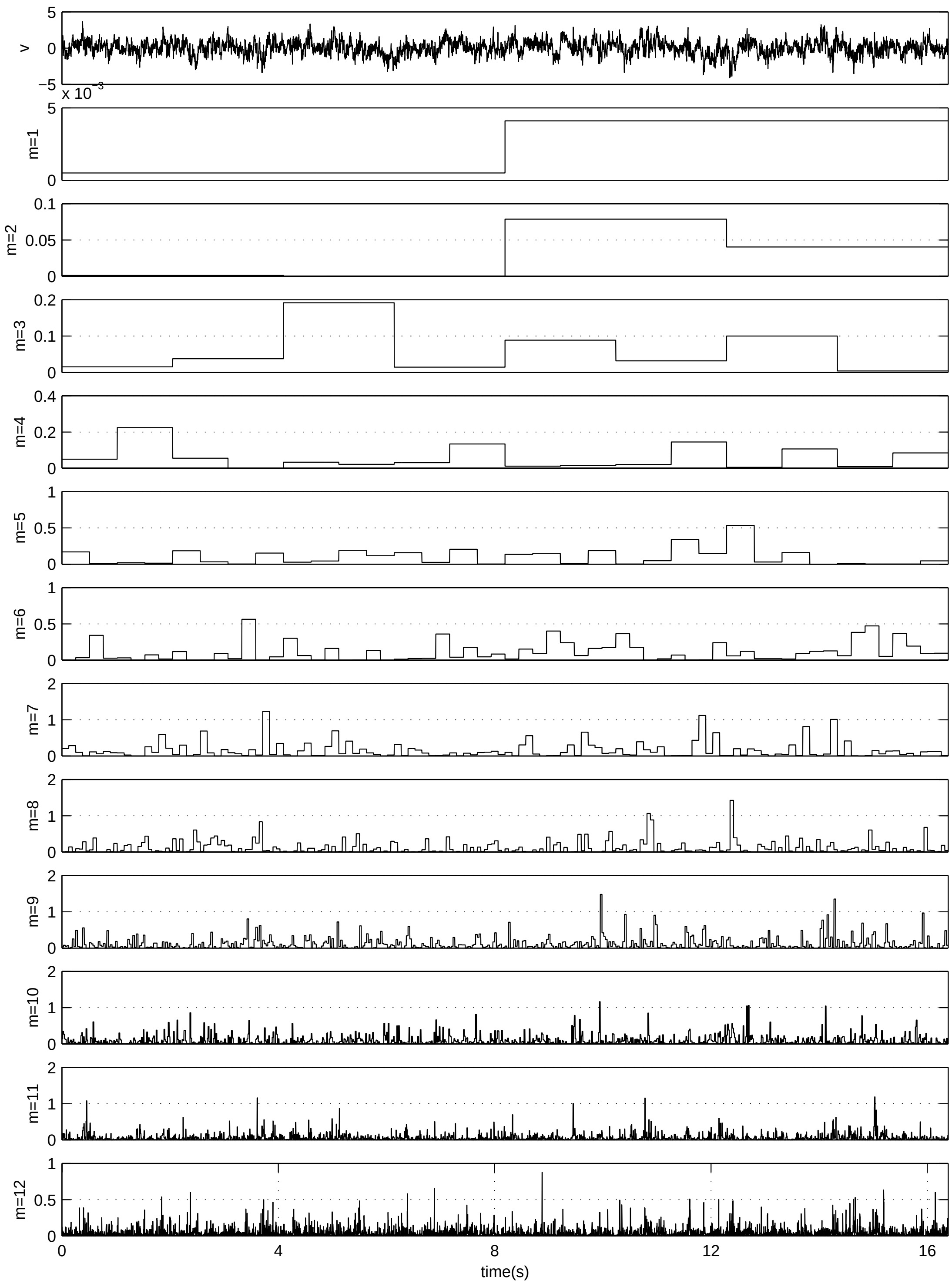

Figure 4.6(a) Wavelet coefficients of u- velocity component of Configuration #6

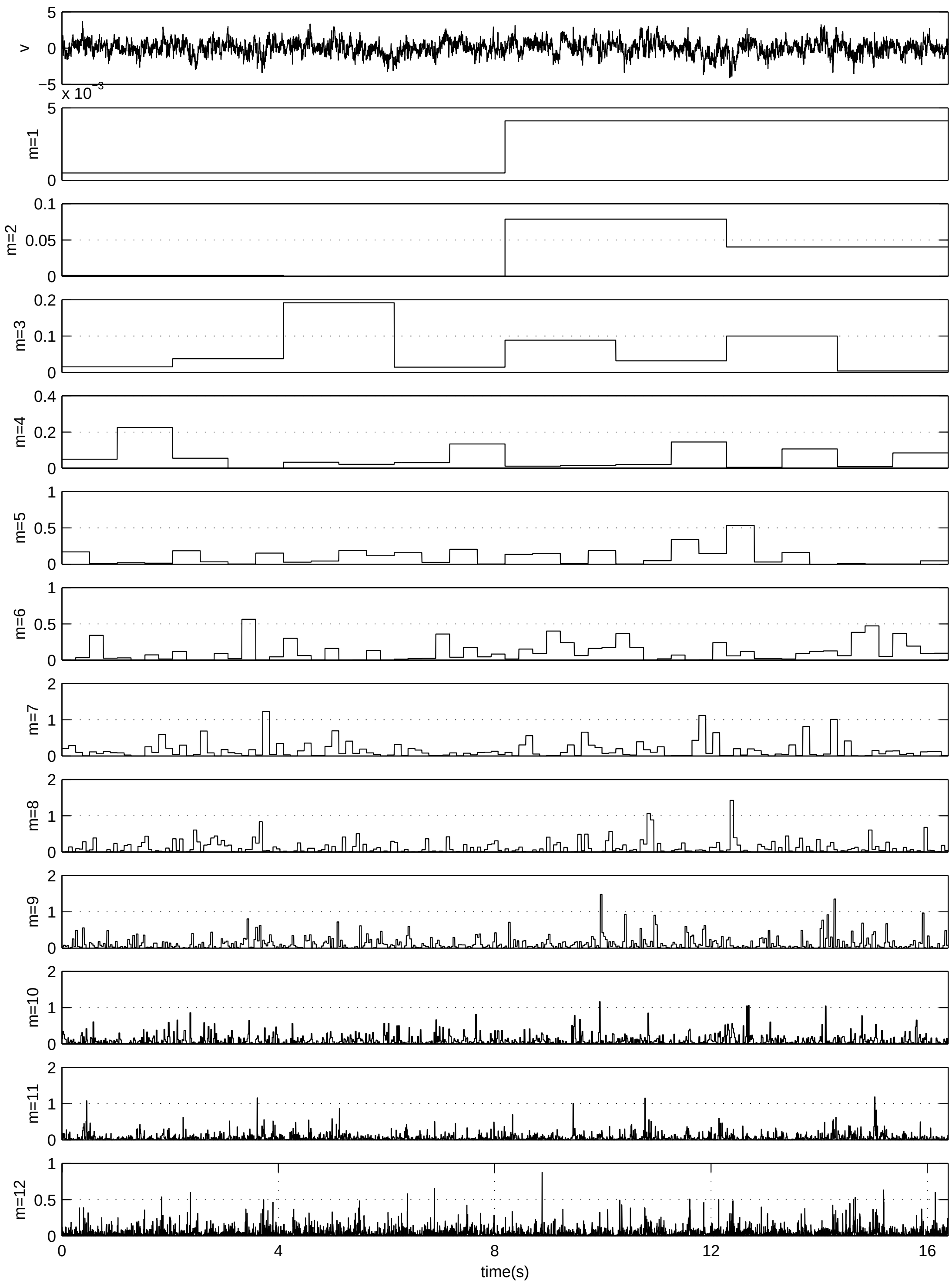

Figure 4.6(b) Wavelet coefficients of u- velocity component of Configuration #6

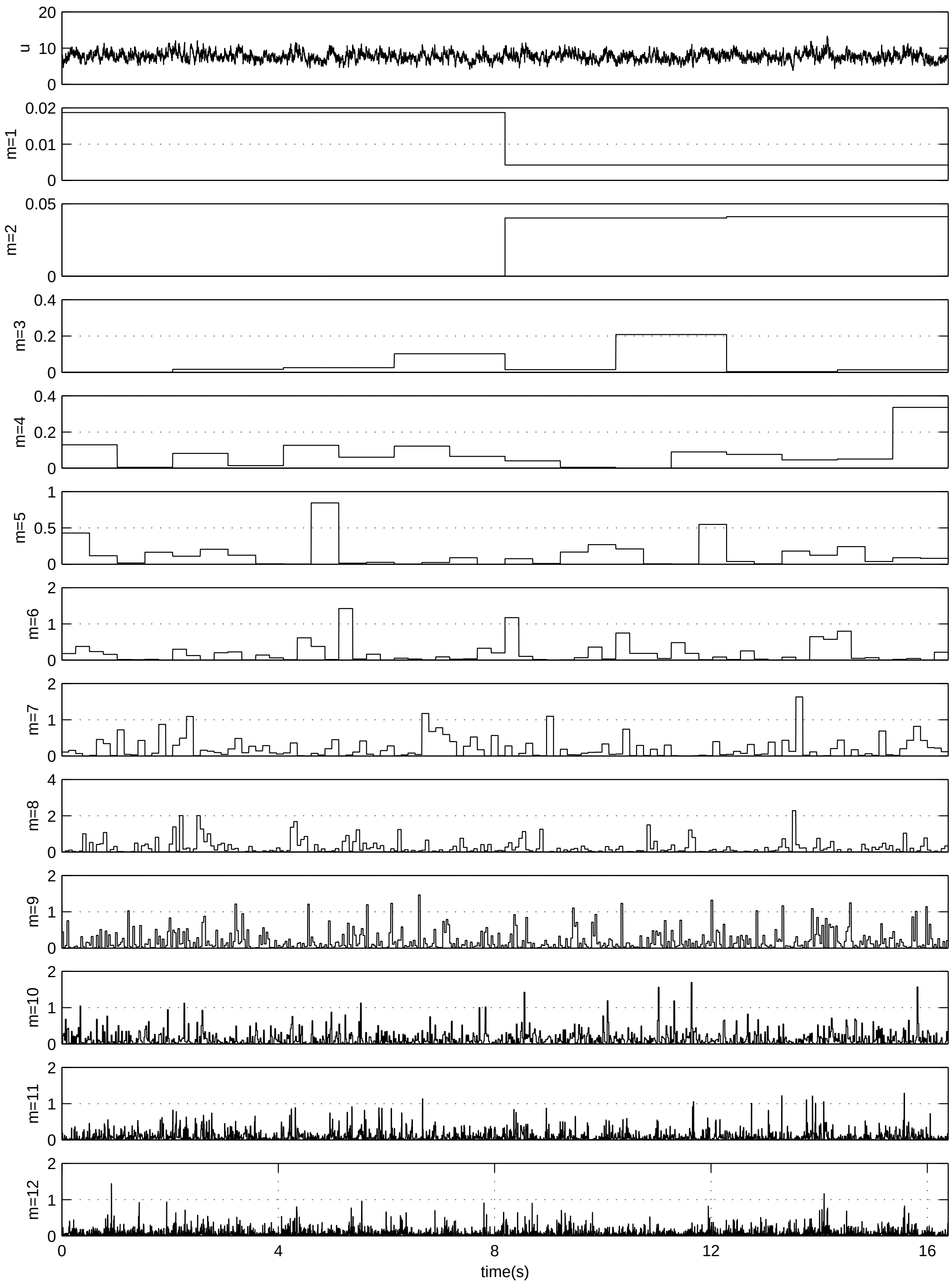

Figure 4.7(a) Wavelet coefficients of u- velocity component of Configuration #7

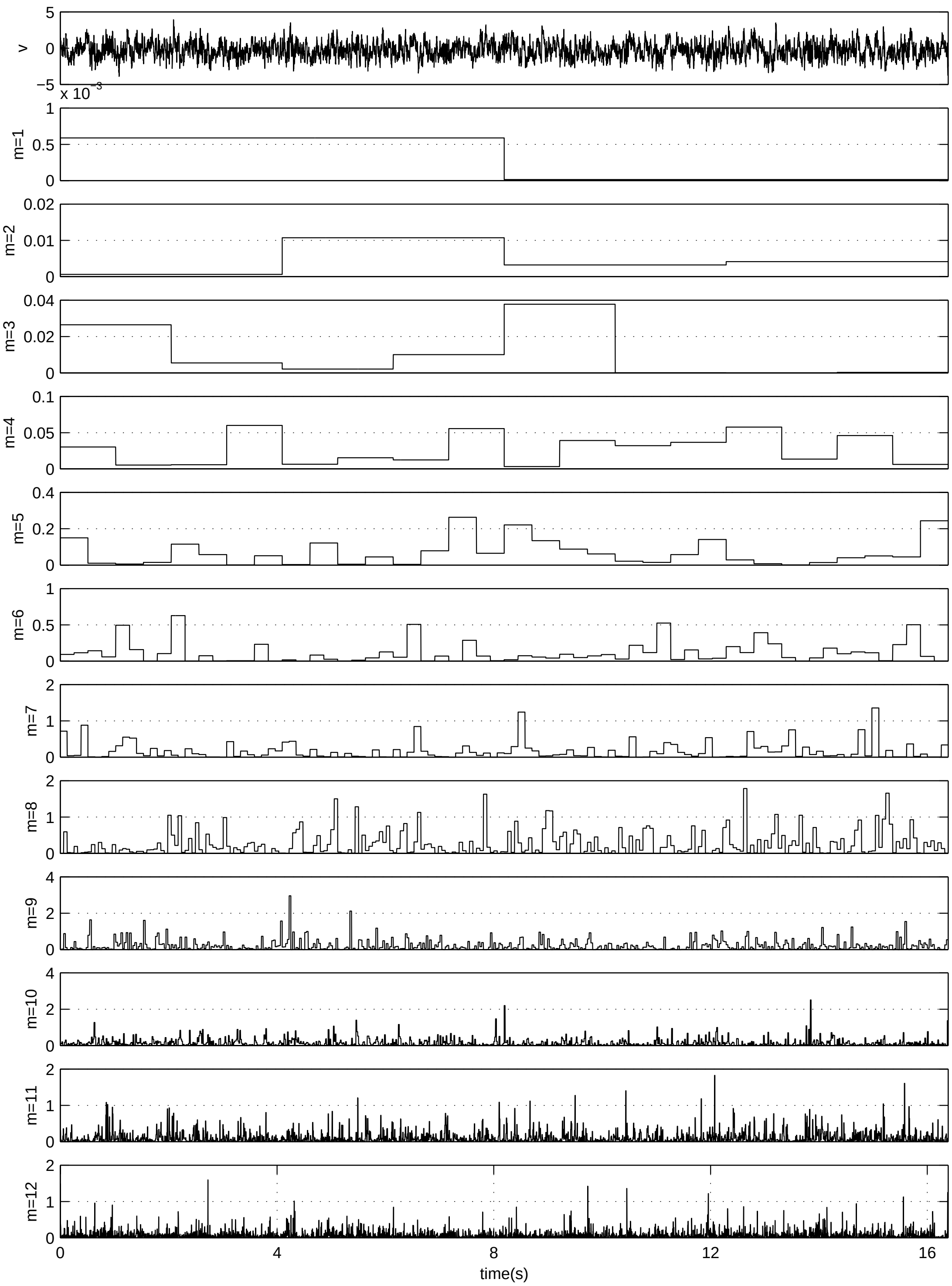

Figure 4.7(b) Wavelet coefficients of v- velocity component of Configuration #7

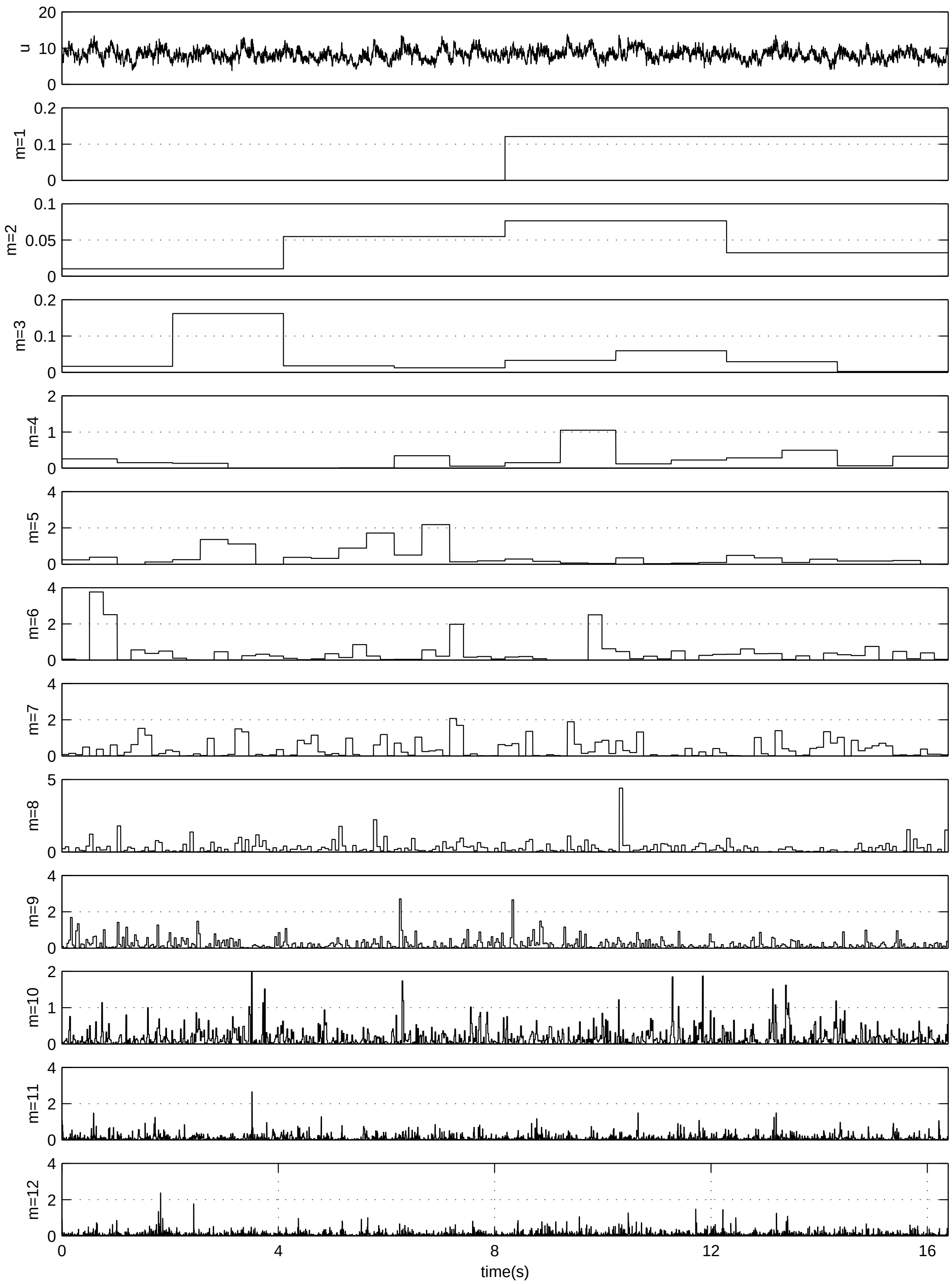

Figure 4.8(a) Wavelet coefficients of u- velocity component of Configuration #8

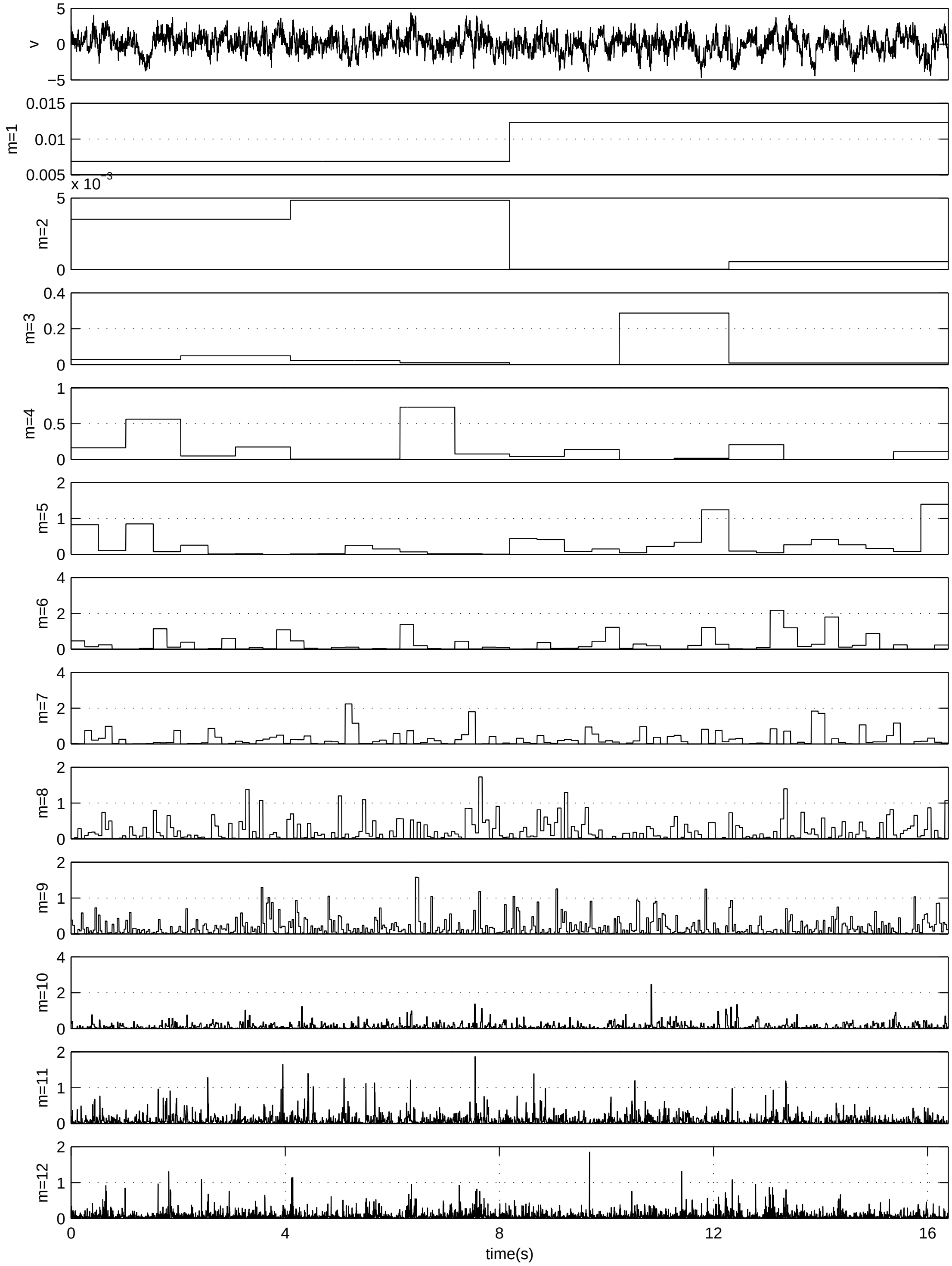

Figure 4.8(b) Wavelet coefficients of v- velocity component of Configuration #8

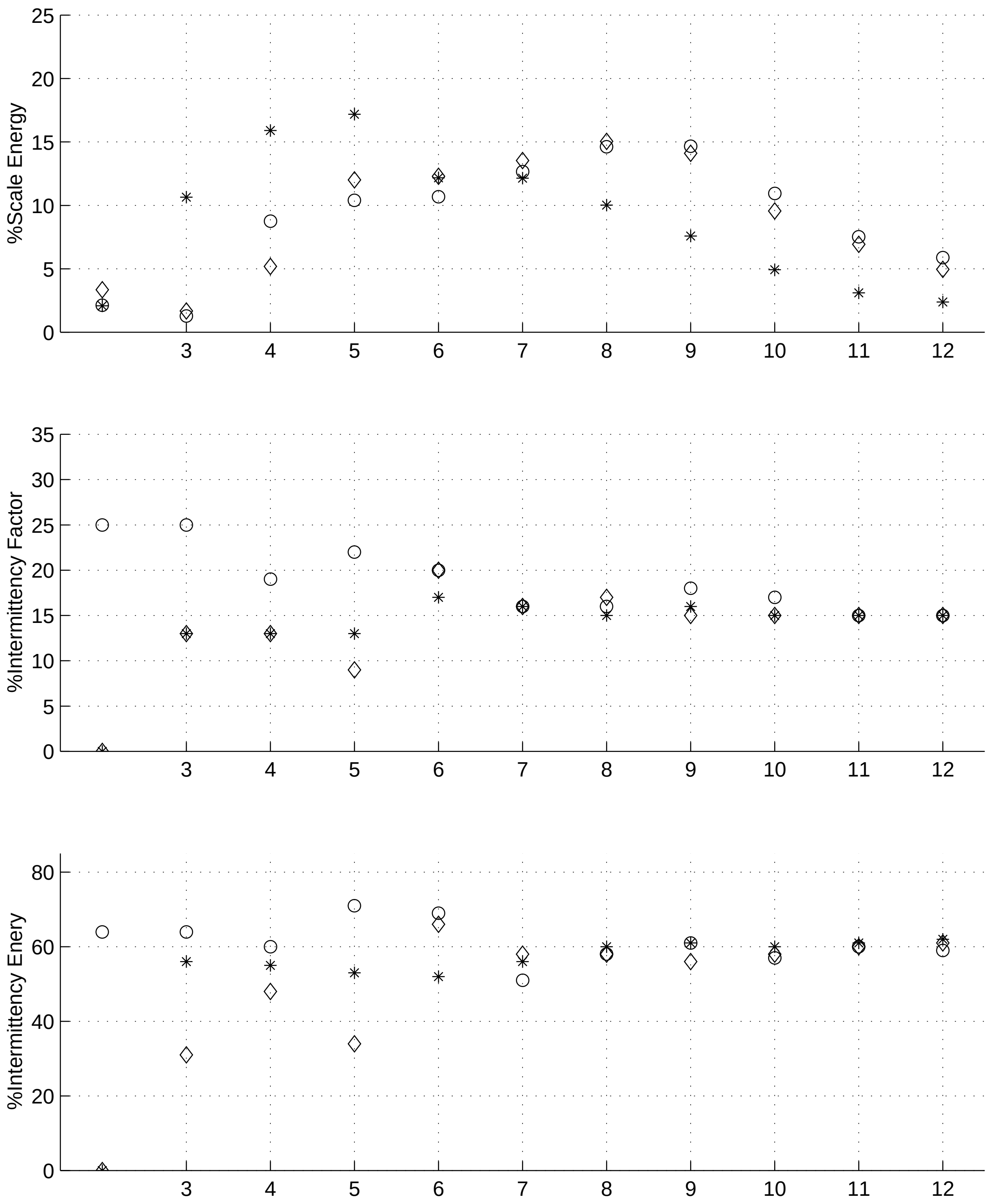

Figure 4.9 Intermittency parameters of u- component : o --- configuration #1,
∗ --- #2, ◊ --- #3, (a) Scale energy (b) Intermittency factor (c) Intermittency energy

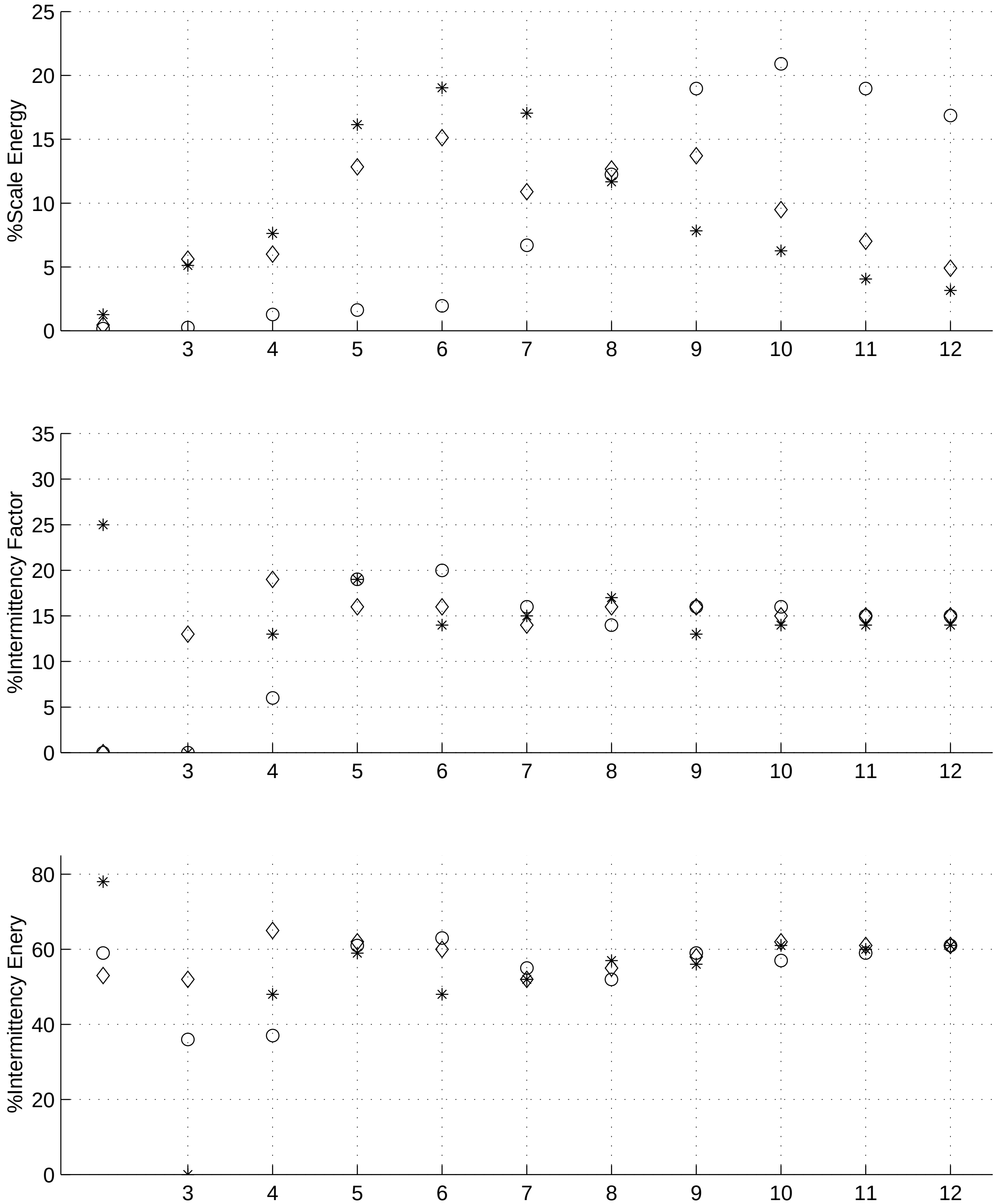

Figure 4.10 Intermittency parameters of v- component : o --- configuration #1,
∗ --- #2, ◊ --- #3: (a) Scale energy (b) Intermittency factor (c) Intermittency energy

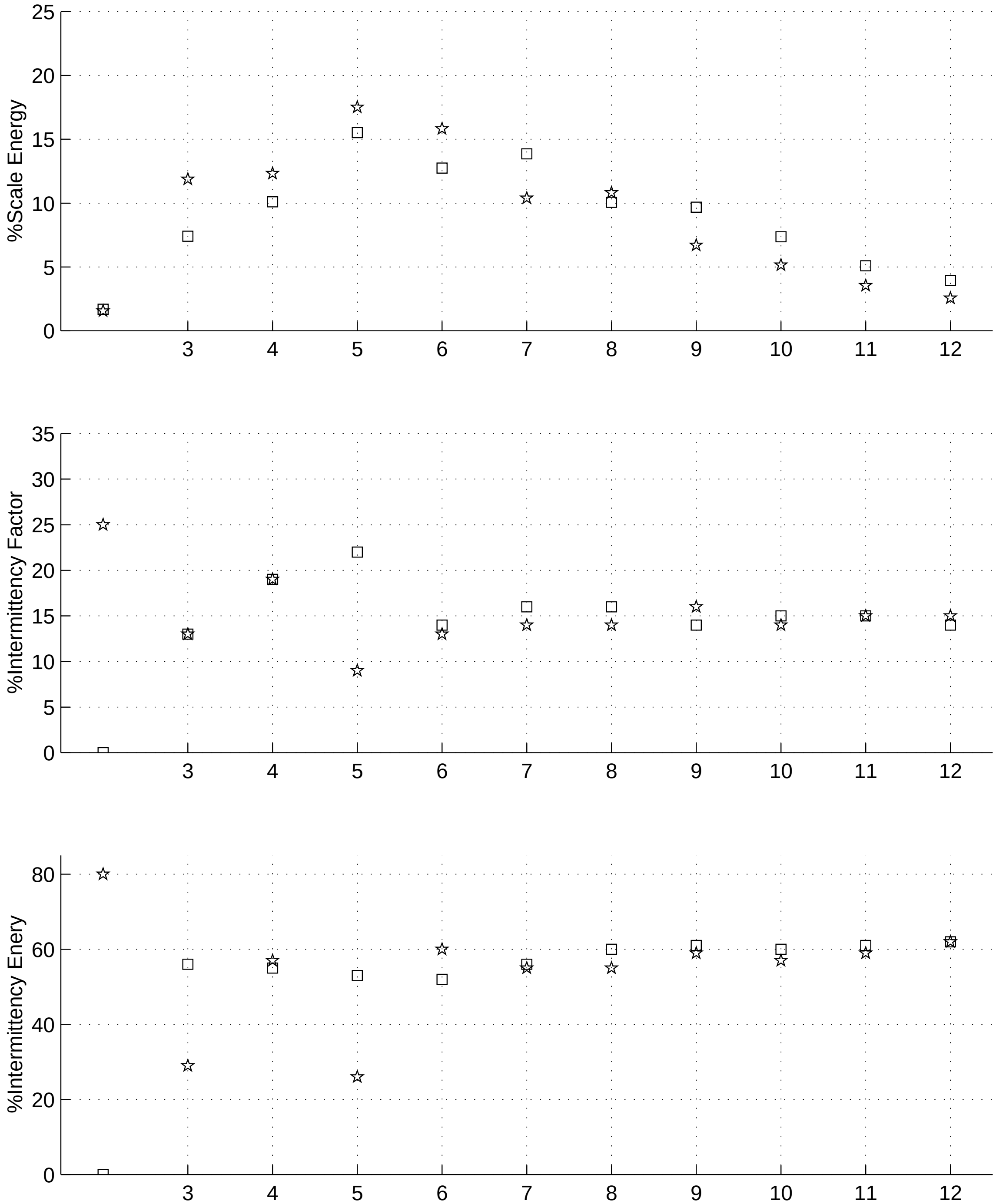

Figure 4.11 Intermittency parameters of u- component : ✰ --- #4, □--- #5: (a) Scale energy (b) Intermittency factor (c) Intermittency energy

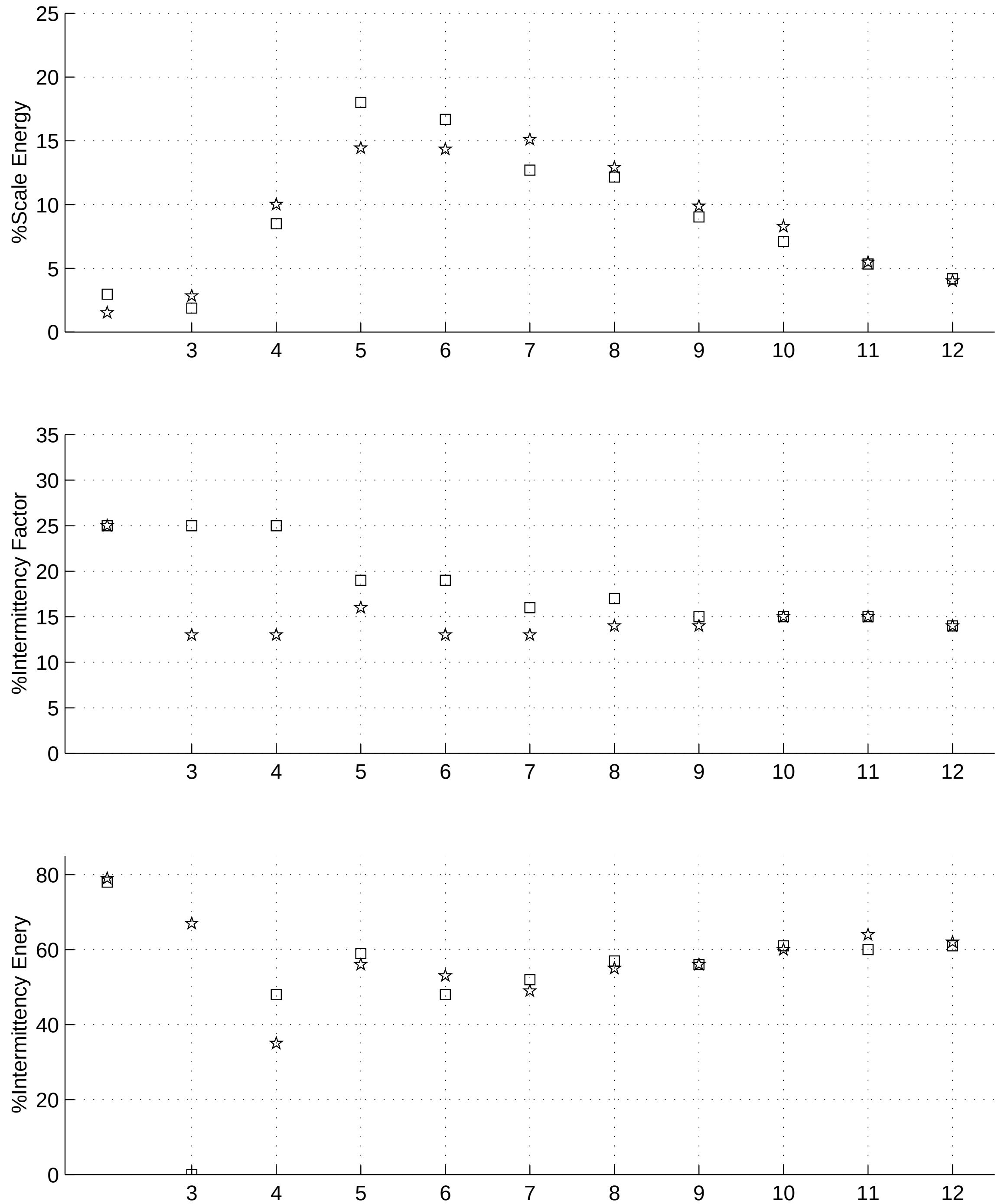

Figure 4.12 Intermittency parameters of v- component: ☆ --- #4, □--- #5: (a) Scale energy (b) Intermittency factor (c) Intermittency energy

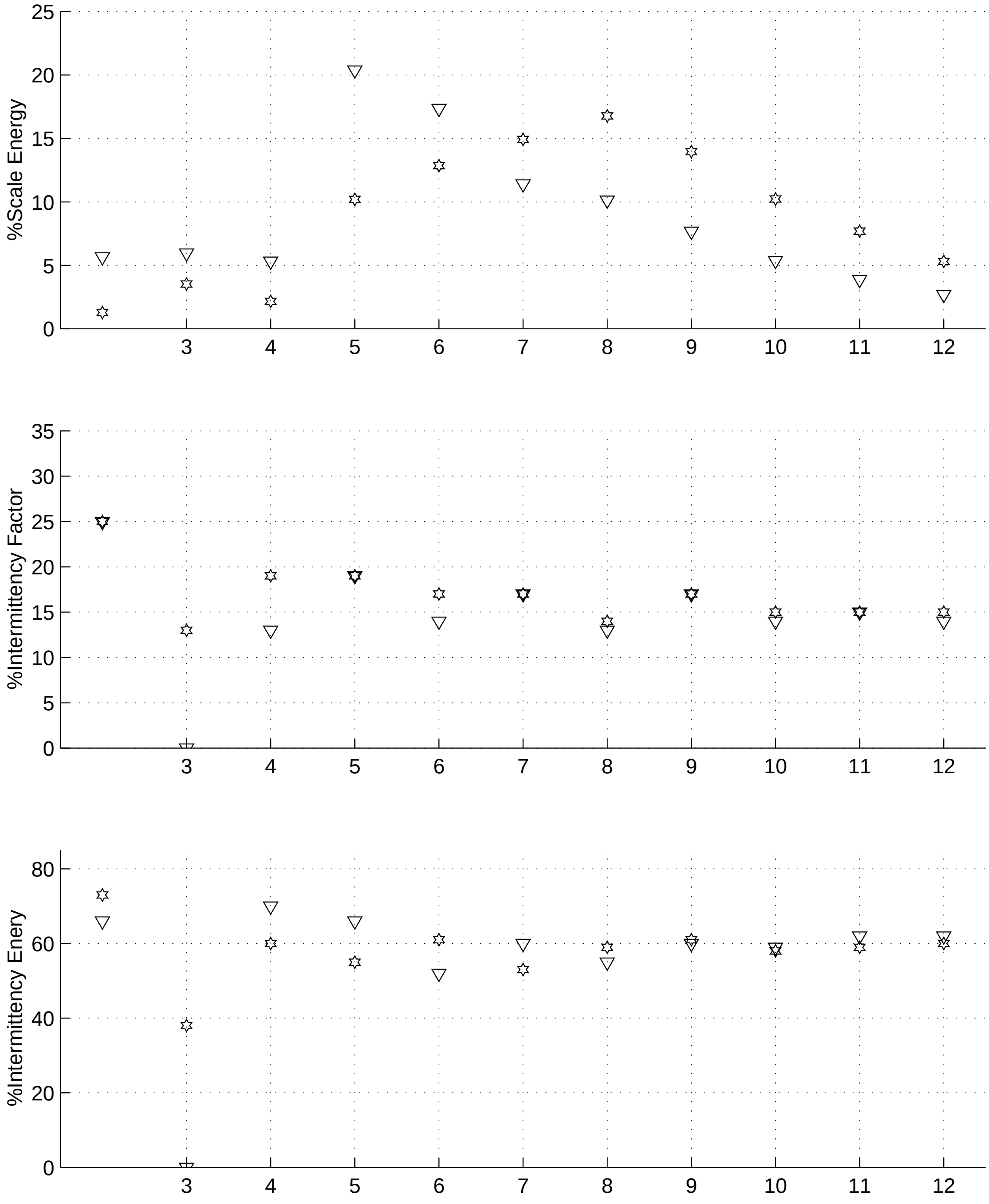

Figure 4.13 Intermittency parameters of u- component ∇ --- #6, ✶ --- #7: (a) Scale energy (b) Intermittency factor (c) Intermittency energy

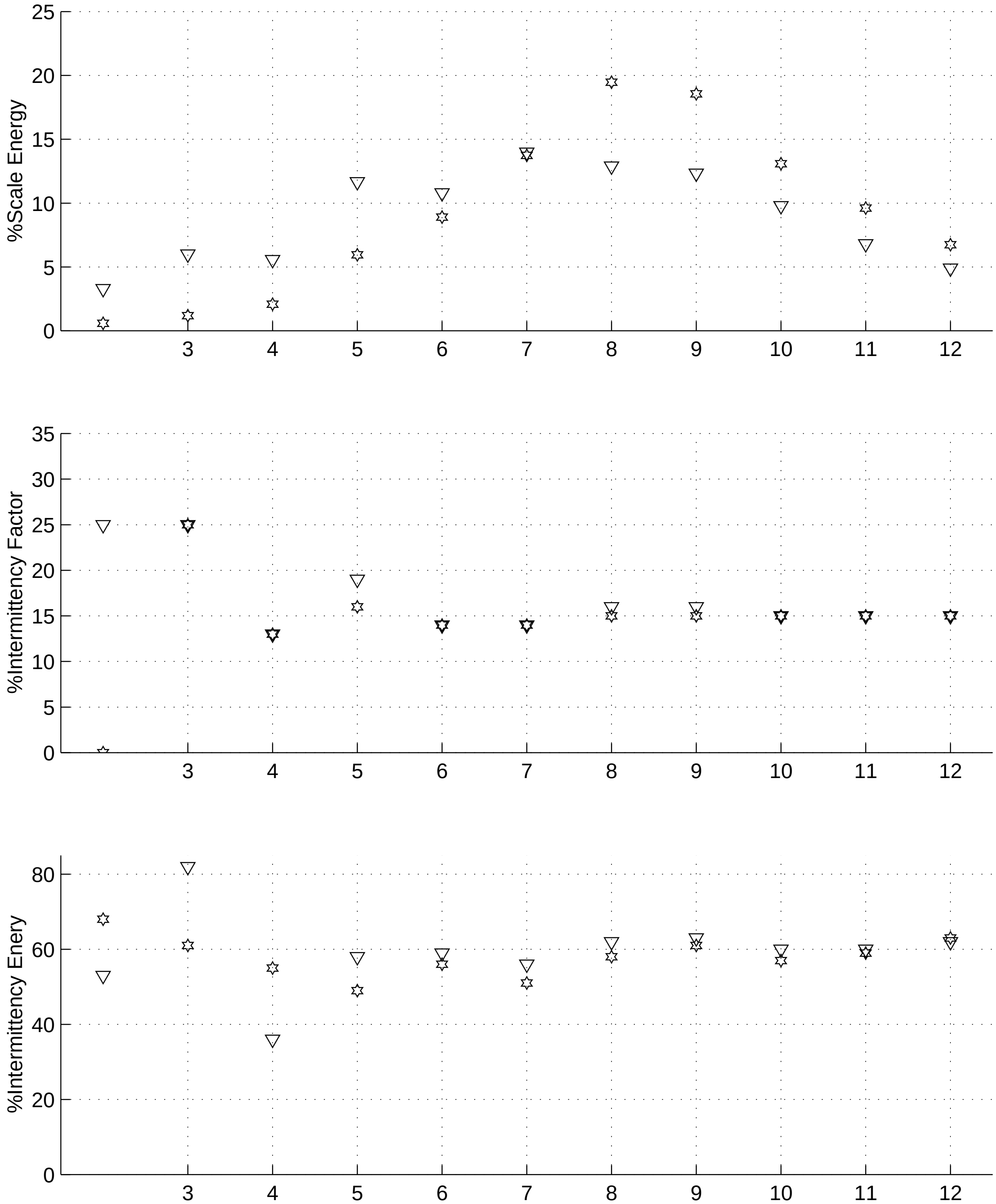

Figure 4.14 Intermittency parameters of u- component: ∇ --- #6, ✶ --- #7: (a) Scale energy (b) Intermittency factor (c) Intermittency energy

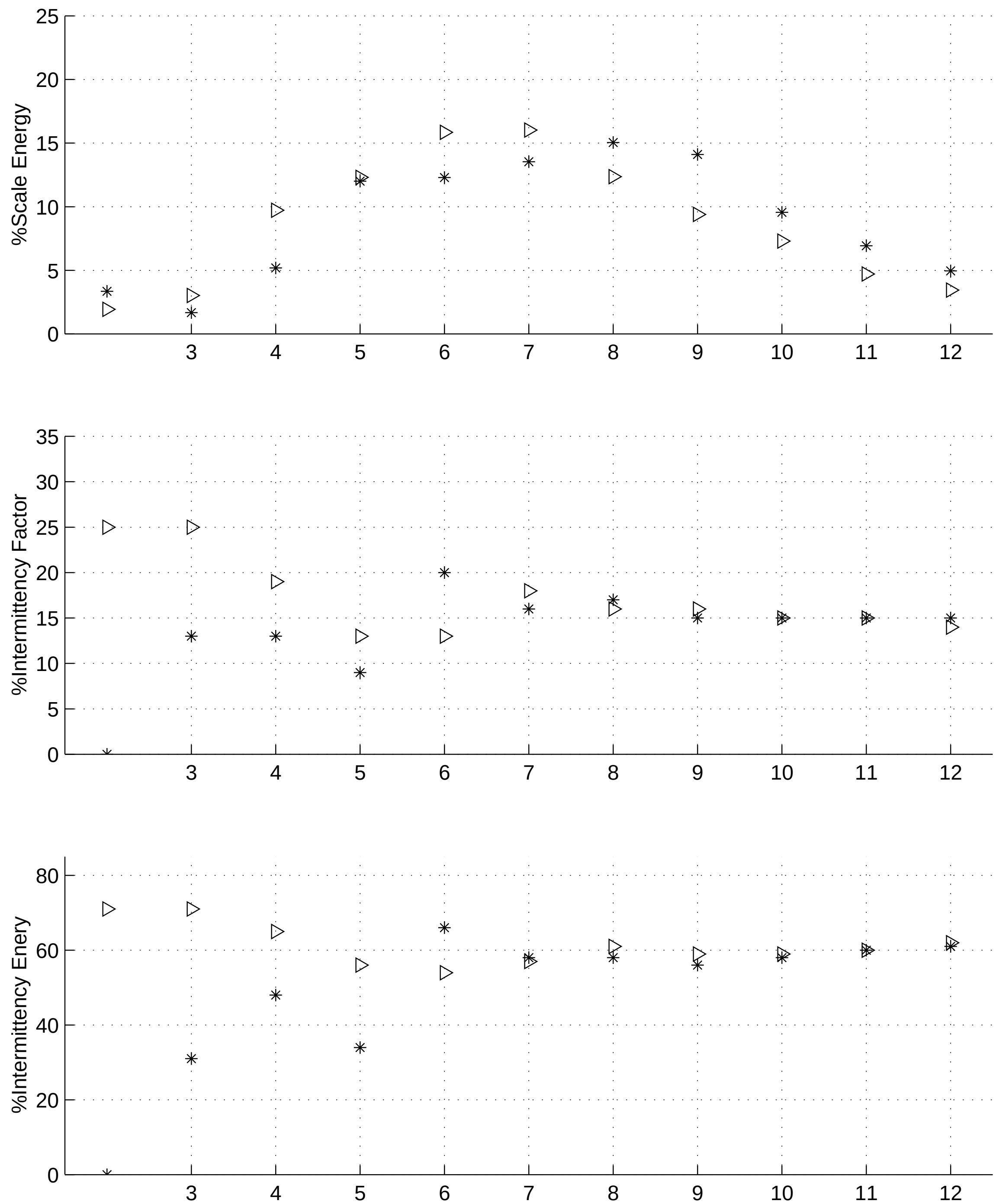

Figure 4.15 Intermittency parameters of u- component: ◊ --- #3, ▹ --- #8: (a) Scale energy (b) Intermittency factor (c) Intermittency energy

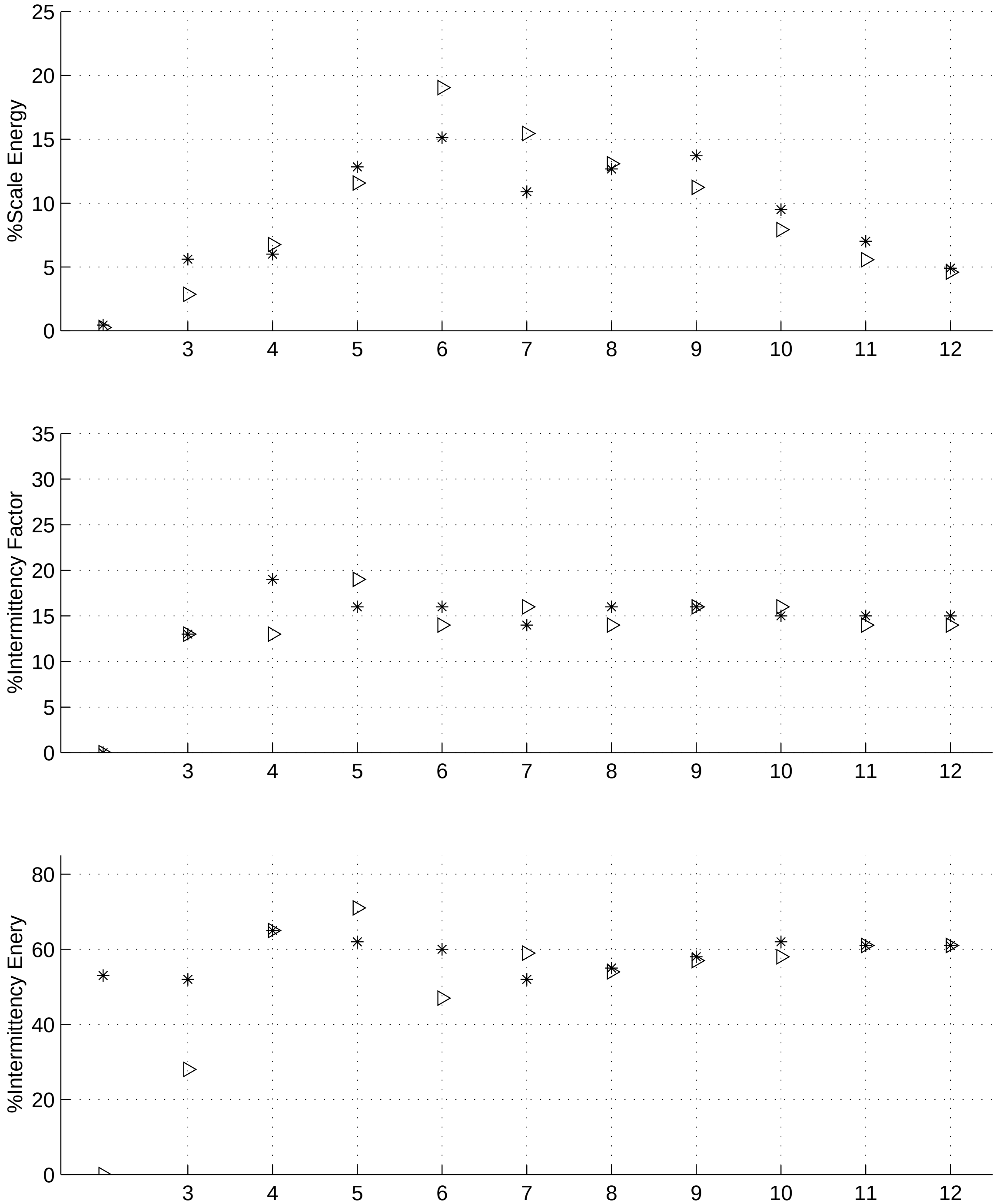

Figure 4.16 Intermittency parameters of v- component: ◊ --- #3, ▹ --- #8: (a) Scale energy (b) Intermittency factor (c) Intermittency energy